FEDERAL UNIVERSITY OF SANTA CATARINA
TECHNOLOGY CENTER
AUTOMATION AND SYSTEMS DEPARTMENT
UNDERGRADUATE COURSE IN CONTROL AND AUTOMATION ENGINEERING

Ícaro Bedôr Jardim Bastos de Paula Cavalcante

Prediction of cutting forces in milling processes using acquired machine tool data for generation of digital twins

Florianópolis
2023

Ícaro Bedôr Jardim Bastos de Paula Cavalcante

Prediction of cutting forces in milling processes using acquired machine tool data for generation of digital twins

Final report of the subject DAS5511 (Course Final Project) as a Concluding Dissertation of the Undergraduate Course in Control and Automation Engineering of the Federal University of Santa Catarina. Supervisor: Prof. Marcelo De Lellis Costa de Oliveira, Dr.

Florianópolis
2023

Ficha de identificação da obra

A ficha de identificação é elaborada pelo próprio autor.

Orientações em:

http://portalbu.ufsc.br/ficha

Ícaro Bedôr Jardim Bastos de Paula Cavalcante

Prediction of cutting forces in milling processes using acquired machine tool data for generation of digital twins

This dissertation was evaluated in the context of the subject DAS5511 (Course Final Project) and approved in its final form by the Undergraduate Course in Control and Automation Engineering

Florianópolis, <month> <day>, <year>.

Prof. Hector Bessa Silveira, Dr.
Course Coordinator

Examining Board:

Prof. Marcelo De Lellis Costa de Oliveira, Dr.
Advisor
UFSC/CTC/DAS

Tommy Venek, Eng.
Supervisor
Company

Prof. xxxx, Dr.
Evaluator
Instituição xxxx

Prof. xxxx, Dr.
Board President
UFSC/CTC/DAS

This work is dedicated to my dear girlfriend, to my admired professors, and to my loving family. The bricks upon the lengthy road that led me here were laid by your hands. I thank you with all my heart.

ACKNOWLEDGEMENTS

I want to thank my girlfriend Dauriane Siqueira for her continued support and encouragement, you were always there for me, all these years. You believed in me from the start, even before myself. Sparing no efforts, you helped me at every step of the way.

My parents, who did everything in their power to give me the best possible education from the start.

My advisor and professor Dr. Marcelo De Lellis for his extensive guidance and orientation, the high quality of this work is a reflection of his excellent teachings and very high standards.

My professor Dr. Frank Steinhoff for believing in me and encouraging me to transfer to my desired university, in pursue of attaining an exchange program to Germany.

My supervisor M.Sc. Tommy Venek for enabling the execution of this work, as well as introducing and guiding me in the field of study of high precision machining.

My supervisor M.Sc. Sven Schiller for his support during the execution of this project, as well as guiding and teaching me in the development of this software.

As well as all my other professors along this journey that inspired me and gave me the background needed to accomplish this milestone. Special thanks to everyone that donated and helped in affording this exchange to Germany.

This project could not have been realized without the help from all these remarkable people.

I cannot overstate my thankfulness.

“It is not knowledge, but the act of learning, not possession but the act of getting there, which grants the greatest enjoyment.”

“Es ist nicht das Wissen, sondern das Lernen, nicht das Besitzen, sondern das Erwerben, nicht das Dasein, sondern das Hinkommen, was den größten Genuss gewährt.”

— Johann Carl Friedrich Gauss (1777 - 1855)

(1000ZITATE, 2022)

DISCLAIMER

Aachen, July 3rd, 2023.

As representative of the **gemineers GmbH** in which the present work was carried out, I declare this document to be exempt from any confidential or sensitive content regarding intellectual property, that may keep it from being published by the Federal University of Santa Catarina (UFSC) to the general public, including its online availability in the Institutional Repository of the University Library (BU). Furthermore, I attest knowledge of the obligation by the author, as a student of UFSC, to deposit this document in the said Institutional Repository, for being it a Final Program Dissertation ("Trabalho de Conclusão de Curso"), in accordance with the Resolução Normativa n° 126/2019/CUn.

Sven Schiller

Sven Schiller
gemineers GmbH

ABSTRACT

This project aims to improve the speed and effectiveness of workpiece quality assurance in milling processes, specifically in assuring that the final machined workpiece conforms to its defined tolerances. To this end, the **company** product software creates a digital twin of the machined workpiece by acquiring process signals during machining, then performing a cutting simulation, where the rotating milling cutter advances along the nominal toolpath, removing material from the workpiece when these geometries intersect. The **company** software is then able to create a 3D geometry colored by the deviations of the resulting simulated workpiece from the nominal desired product geometry. During milling, the forces needed to cut the metal workpieces are considerably high, which can cause the cutting tool to bend and deflect. This project presents an improvement of the **company** digital twin generation by predicting the process forces felt by the cutting tool when removing material from the workpiece, then simulating the deflection of the cutting tool along the toolpath. To do this, the acquired signals need to be thoroughly and properly filtered, as their quality and reliability can vary significantly. The process of choosing a proper filter for the architecture is thoroughly described, based on a mixed quantitative and qualitative analysis. Subsequently, a deeper tool contact with the workpiece simulation is developed. The result of this simulation allows for the calculation of more significant properties of the corresponding cutting force. The use this improved simulation augments the overall fidelity of the simulation, creating a digital twin that better represents its real counterpart, as well as generating profound information about the physical process that cannot be, or is difficult to acquire.

Keywords: Digital twins. Milling. Digital signal processing. Force modeling. Force prediction. Quality assurance.

RESUMO

Este projeto tem como objetivo melhorar a velocidade e eficácia da garantia de qualidade de peças em processos de fresagem, especificamente, assegurando que a peça usinada final esteja dentro das tolerâncias definidas. Para isso, o software da empresa cria um gêmeo digital da peça usinada, adquirindo sinais do processo durante a usinagem e realizando uma simulação de corte, na qual a fresa rotativa avança ao longo da trajetória nominal da ferramenta, removendo material da peça quando essas geometrias se intersectam. O software da empresa é capaz, então, de criar uma geometria 3D colorida pelos desvios da peça simulada em relação à geometria nominal desejada. Durante a fresagem, as forças necessárias para cortar as peças são consideravelmente altas, o que pode fazer com que a ferramenta de corte se curve e se desvie. Este projeto apresenta uma melhoria na geração de gêmeos digitais da empresa, ao prever as forças de processo sentidas pela ferramenta de corte ao remover material da peça e, em seguida, simular a deflexão da ferramenta ao longo de sua trajetória nominal. Para isso, os sinais adquiridos precisam ser filtrados de maneira minuciosa e adequada, pois sua qualidade e confiabilidade podem variar significativamente. O processo de escolha de um filtro adequado para a arquitetura é descrito detalhadamente, com base em uma análise quantitativa e qualitativa combinada. Posteriormente, é desenvolvida uma simulação de contato da ferramenta com a peça. O resultado dessa simulação permite o cálculo de propriedades mais significativas da força de corte correspondente. O uso desta simulação aprimorada aumenta a fidelidade geral da simulação, criando um gêmeo digital que representa melhor sua contraparte real, além de gerar informações detalhadas sobre o processo físico que não podem ser adquiridas ou são difíceis de serem obtidas.

Palavras-chave: Gêmeos digitais. Usinagem. Processamento digital de sinais. Modelagem de forças. Previsao de forças. Garantia de qualidade.

LIST OF FIGURES

LIST OF TABLES

LIST OF ABBREVIATIONS AND ACRONYMS

FIR	Finite Impulse Response
IIR	Infinite Impulse Response

LIST OF SYMBOLS

v_f	Linear speed of the tip of the cutting tool
ω	Angular speed of cutting tool
R_0	Cutting tool nominal radius
h_{sp}	Chip thickness
b_{sp}	Chip width
l_{sp}	Chip length
A_{sp}	Chip cross sectional area
λ	Nominal helix angle of the cutting tool
a_e	Step over
a_p	Depth of cut
f_z	Feed per tooth

CONTENTS

INTRODUCTION

The activities reported in this document were carried out during a one year internship at a software company. The main objective of the **company**, as it will be further explained later in this report, is the construction and development of Digital Twin technology for machining processes, aiming to achieve a perfect digital representation of both the workpiece and the machine tool throughout the whole milling process. In this context, the main product of the **company** is a software architecture that is divided in different areas, each one specialized in a part of the process in the creation of the Digital Twin, of the process and workpiece.

Information about the machining process is acquired form machine tools, filtered, processed and visualized in the software.

This project was developed by the student in the data processing branch of the software, it is a continuation of his previous work done in this **company** during his internship, which will also be reviewed later in this document. This report introduces the reader to machining processes, followed by a study of the state of the art, and a review of the past work done by the student. After this initial introduction, the work done by the student will be presented in detail.

PROJECT GOAL

The objective of this project is to create a fitting cutting forces prediction algorithm for milling processes, by using machine tool acquired signals and simulation data to infer and extrapolate information about the cutting process. In order to employ the acquired machine tool signals into the simulations, the signals must be properly and thoroughly filtered beforehand.

In summary, the goal of this project is to create an algorithm for creation of an as accurate as possible digital twin geometry of a milled workpiece, that works reasonably well for the widest range of process parameters and machine tool manufacturers.

1 BACKGROUND

The first chapter of this work aims to give the reader a background on milling processes, digital twins, the **company**, the project and the internship, followed by an overview of the scope and structure of the project report.

1.1 MILLING PROCESSES

Milling is the process of machining using a rotating cutting tool, advancing it into the workpiece to remove material. A milling process applies many small cuts to the workpiece, each removing a small amount of material, cutting down the piece into the desired shape. The removed material from one of these small cuts is called a chip. These many small cuts are attained by a combination of the milling tool containing multiple sharp teeth, rotating the tool at high speeds, and advancing slowly through the material. The speed of the cutter through the material is called the feed rate, and the rotational speed of the tool is called the spindle speed. The quality of the resulting workpiece depends on both of these parameters throughout the cutting process, as well as the tool shape and workpiece material.

The Figure 1 shows a simplified view of a modern high performance milling process:

Figure 1 – Simplified view of a high performance milling Process.

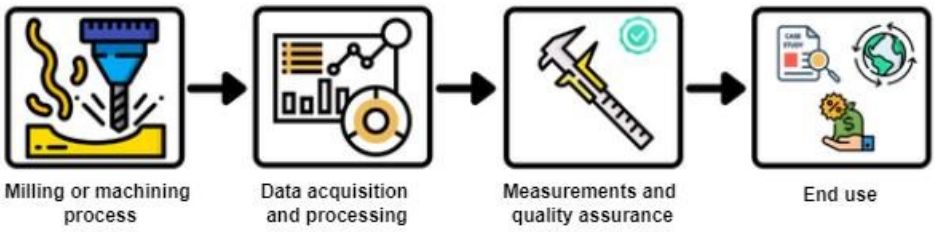

Source: **Company**'s Archive.

1. The machine starts the actual machining process aided by a Computer Numeric Control (CNC);
2. During the process, machine data can be acquired and processed in order to better analyze and understand the process. In the case of the **company**, the machine data will be used to simulate and construct a digital twin of the process;
3. After the machining process is finished, the piece should go through a rigorous measurement process in order to assure that that its shape lies within its tight tolerance bounds;
4. After the piece's quality has been assessed, the process is complete and the piece can go on to its final use. Otherwise, it can be either discarded or reworked.

1.2 DIGITAL TWIN TECHNOLOGY

A digital twin is a digital representation of a physical process or object, that can then be used to run simulations, to make predictions of performance and quality, or to analyze in real time the state of a complex physical system. According to IBM (2022):

> "A digital twin is a virtual model designed to accurately reflect a physical object. The object being studied — for example, a wind turbine — is outfitted with various sensors related to vital areas of functionality. These sensors produce data about different aspects of the physical object's performance, such as energy output, temperature, weather conditions and more. This data is then relayed to a processing system and applied to the digital copy.
>
> Once informed with such data, the virtual model can be used to run simulations, study performance issues and generate possible improvements, all with the goal of generating valuable insights — which can then be applied back to the original physical object."

1.3 RESEARCH PROBLEM

The purpose of this project arises from the **company** necessity of having a digital twin of a milling process that is as similar as possible to its real counterpart. During a milling process, a quickly rotating edged cutting tool advances into a workpiece cutting and removing material.

Although many optimizations can be done in the milling process itself to try and guarantee its conformity to its tolerances, the workpiece still has to be measured after machining ends. The measurement process is expensive, time consuming and can be made difficult depending on the geometry of the workpiece. Many of these problems could be lessened if the companies had access to the localized workpiece deviations from the nominal geometry before measurement, as this would allow the operator to know beforehand which regions of the workpiece need to be worked on, which regions need to be measured and which should be conforming to the tolerances. By just reducing the regions of the workpiece that need to be measured would entail in high benefits for most high performance machining applications.

This use case is the core of the **company** platform, where it uses acquired machine data from the machining process, in order to evaluate, infer, extrapolate and predict information about the final workpiece, and about the process itself.

SCOPE AND STRUCTURE OF THIS REPORT

This report is divided into chapters in the following structure:

- Chapter 1 - Background
  Quick overview of milling processes, digital twins, the company, the project objective and the report structure.

- Chapter 2 - State of the art
  Theoretical basis for the project, as well as a brief explanation of the technologies and models used for this work.

- Chapter 3 - Review of previous work
  A short review of what was previously developed by the student. As this project is a continuation of the previous work, it is important for the reader to understand the foundation of the entire project, as well as being reminded of previous results.

- Chapter 4 - Filtering of process signals
  Description of the first phase of the project, that is, researching, analyzing, testing and making a decision on what filter to apply to the acquired machine signals.

- Chapter 5 - Force modeling
  Development of the tool cutting edge contact simulation for deeper analysis of cutting forces.

- Chapter 6 - Experimental validation
  Testing the developed simulations with experimental data acquired from real milling processes.

- Chapter 7 - Conclusion
  A review of what has been achieved, possible improvements, future work.

2 STATE OF THE ART

This chapter presents the technological basis of this project, its theoretical foundation, the relevance of the problem this project tries to solve, the importance of finding a solution for said problem, and the applicability of this project. All the cutting tool geometries that are mentioned or used in this project are presented in Appendix 6, together with a brief explanation of their corresponding main use in a milling process.

2.1 THEORETICAL FOUNDATION

The first phase of this work, which consists in the filtering of the necessary process signals for the force prediction algorithm, employs different signal processing methods, such as Infinite Impulse Response (IIR) filters and Finite Impulse Response (FIR) filters.

IIR filters

This is the type of filter most commonly used in the Control and Automation engineering graduation. These are filters whose impulse response can only asymptotically approach zero, as contains feedback in its output, that is, the output of this filter depends not only on previous inputs, but also on previous outputs, meaning that IIR filters can also be unstable. The transfer function of this type of filter always contains a non-trivial denominator, which are the feedback terms. IIR filters are frequently used in practice in engineering as they can be built out of electrical components, such as resistors, capacitors and inductors, and can also be implemented digitally.

FIR filters

This type of filter differs from IIR by having an impulse response that settles to zero after some time or number of samples. These filters employ no feedback, and as such, are inherently stable. A FIR filter is usually implemented digitally by applying a discrete convolution of a chosen window function with the desired signal to be filtered. By doing this, the window function is effectively the impulse response of the digital filter, thus making it simple to design a FIR filter with a desired impulse response, as this impulse response need only to be implemented as the window function for the filter.

The main disadvantage of FIR filters is its computational efficiency, as generally a lot less calculations are needed to filter a signal when using a digital IIR filter, as the order of a FIR filter is the size of the window function. However, their main advantages over IIR filters are the stability and simplicity of designing of a filter with a chosen impulse response. The window functions that were used in this project can be seen in Appendix 6.

Geometry of a milling process

In order to analyze the industry standard physics-based force models, we must first present the geometrical parameters of a milling process, namely the macroscopic contact geometry, the uncut chip geometry and the geometry of the tool's cutting edges. Starting by exploring the macroscopic contact conditions.

The parameters utilized in this work can be seen summarized in Figure 2, with a description of its parameters in Table 1. These technological parameters are measured or estimated from the translational movement of the tool in relation to the workpiece, not considering its rotation around its own axis (CABRAL, 2015).

Figure 2 – Macroscopic contact conditions of a milling process with an end milling tool.

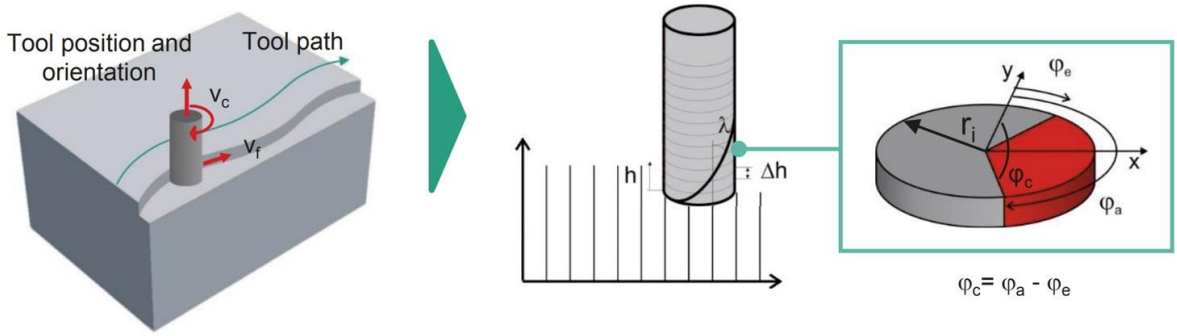

Source: Cabral (2015).

Table 1 – Nomenclature for the macroscopic contact variables

Variable	Name	Description	Usual units
v_f	Feedrate	Linear speed of the tooltip in relation to the workpiece	mm/min
ω	Spindle speed	Rotational speed of the cutting tool	rpm
λ	Helix angle	Nominal helix angle of the cutting tool	degree
r_i	Local radius	Radius of the cutting tool at the discretized slice i	mm
R_0	Nominal radius	Nominal radius of the cutting tool	mm
Φ_e	Entrance angle	Angle at which the contact between the tool and workpiece begins	degree
Φ_a	Exit angle	Angle at which the contact between the tool and workpiece ends	degree
A_{surf}	Chip surface area	Total surface area of the engagement region	degree

Source: Personal archive

Other very important technological parameters of a milling process are the feed per tooth f_z, the linear distance that the tool travels for each tooth pass, the depth of cut, the axial depth of the tool in contact with the material, and the step over, which is

the orthogonal distance between two consecutive tool passes on the same region. If the milling tool contains N teeth, the feed per tooth is calculated with $f_z = \frac{v_f}{\omega N}$.

As the tool follows the tool path while rotating around itself, the tip of each of its cutting edges traces a cycloidal path. A cycloid is the curve that results from a superposition of a rotational movement with a translational movement, this curve can be seen in Figure 3. The uncut chip geometry is defined by the volume of workpiece material removed by a single edge pass, that is, it is the geometry generated by two consecutive edge passes intersected with the workpiece geometry.

The uncut chip geometry is mainly described by four parameters:

- **Chip thickness** h_{sp}, which is the radial length of the chip measured in the direction perpendicular to the local tool surface.
- **Chip width** b_{sp}, which is the cutting edge length in contact with the chip.
- **Chip length** l_{sp}, which is the length measured along the tangential direction of the tool surface.
- **Chip cross sectional area** A_{sp}, which is the area of the chip projected onto the cutting edge surface.

Figure 3 – Uncut chip thickness and cycloidal edge trajectory.

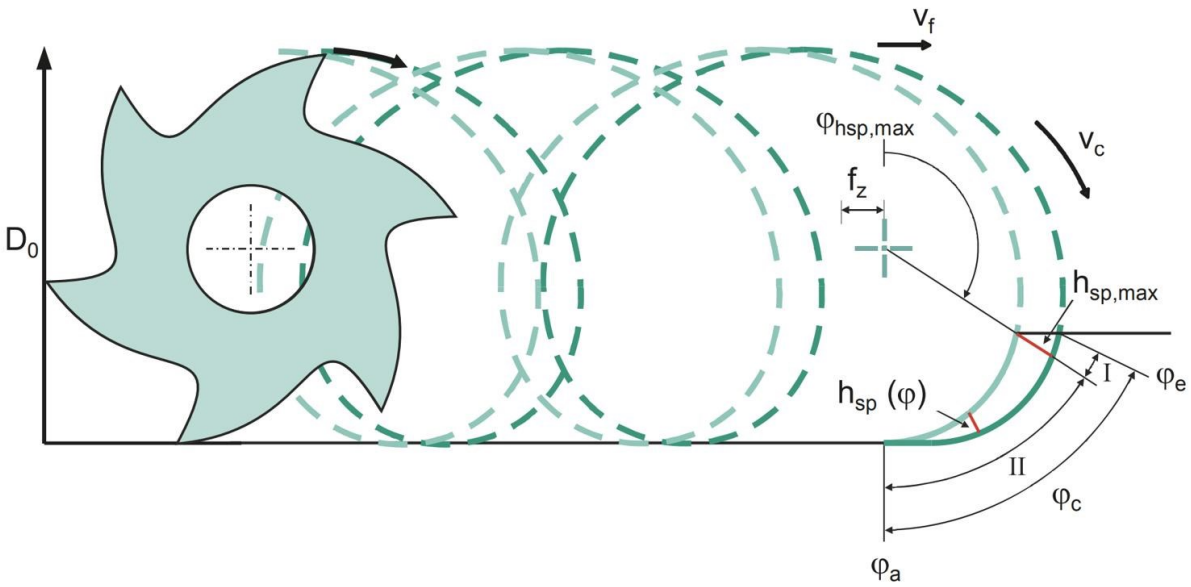

Source: Cabral (2015).

Figure 4 – Uncut chip geometry, and the cutting edge geometry in the 2D tool surface coordinate system.

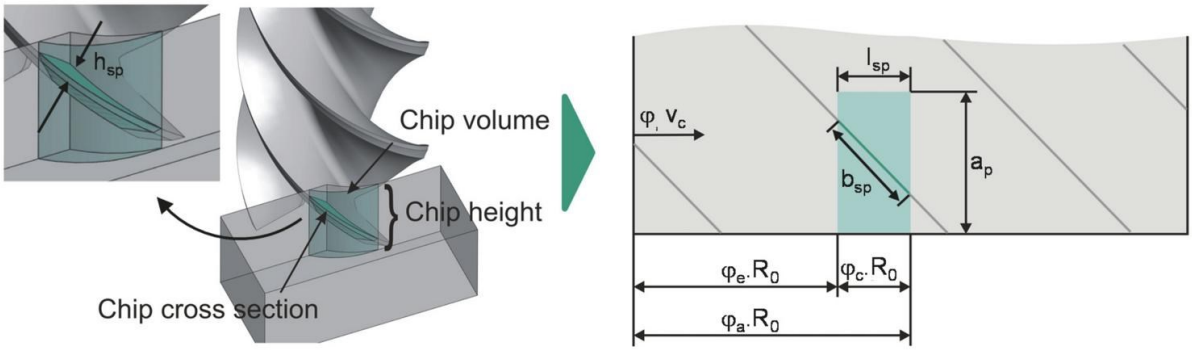

Source: Cabral (2015).

2.2 RELEVANCE OF THIS PROJECT

This project aims to improve the fidelity of the quality prediction results of the **company** platform by improving its force prediction algorithm, allowing it to generate a finer, deeper prediction of the forces present in a milling process. As the force prediction improves, the simulated tool behavior becomes closer to reality, making the simulated machined workpiece become more representative of its real counterpart by taking into account the deflection of the cutting tool.

This way, the results presented in this project can be immediately applied in the **company** software platform.

3 SIGNAL PROCESSING

This chapter presents the continuation of the previous work and the second phase of the overall milling quality prediction project, being developed in the second half of the student's year of internship in the **company**. The work developed by the student was separated in 4 smaller phases, each one depending on the result of the previously executed one. The phases were presented in the introduction, but now the reader should be able to better envision their execution, as their theoretical basis was explained previously.

1. To filter the input load signal
2. To create a force prediction simulation
3. To compare the signal with the simulation output
4. To experimentally validate the model

This chapter presents the first phase of this project, which consists of the research and analysis of a proper filtering pipeline for the acquired load signal.

FILTERING OF THE LOAD SIGNAL

The quality of the acquired load signal depends strongly on the manufacturer of the machine tool. For some manufacturers the signal can be used as acquired, but for others the acquired signal may contain too much high frequency noise, as well as low frequency temperature drifts, and an idle load can be caused by high rotational speeds.

Figure 5 – Acquired load signal from example **A**, presenting a low SNR.

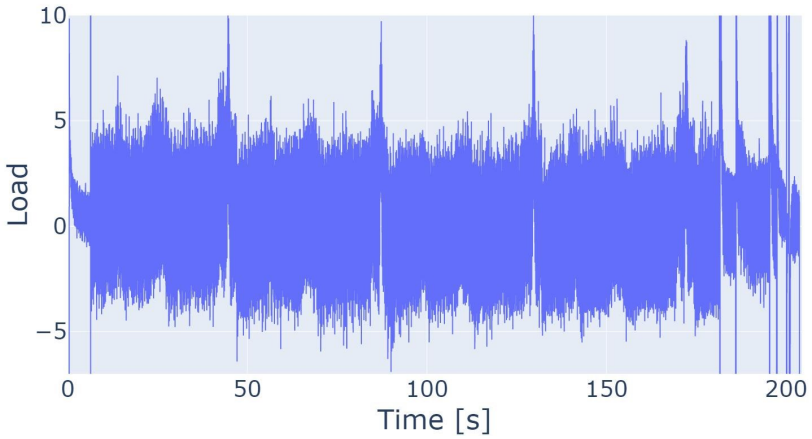

Source: **Company**' archive.

Figure 6 – Acquired load signal from example **B**, presenting a low SNR, high idle load and temperature drift.

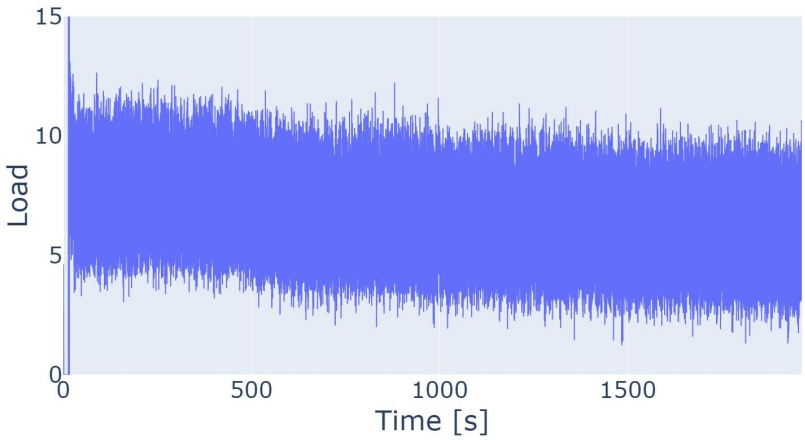

Source: **Company**' archive.

Figure 7 – Acquired load signal from example **C**, presenting a good SNR and practically no idle load.

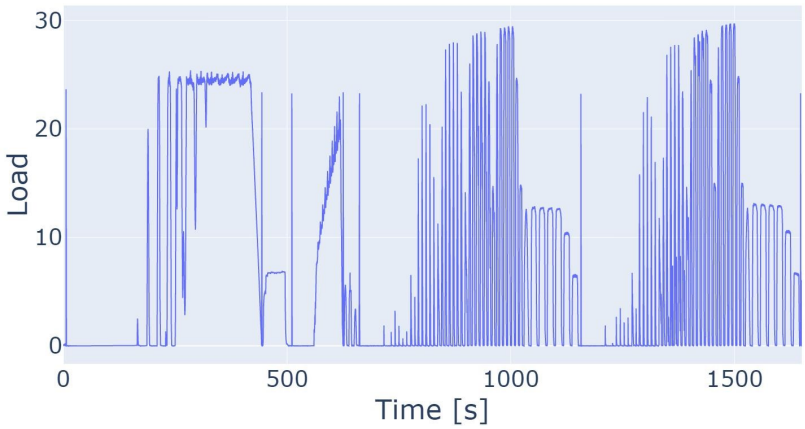

Source: **Company**' archive.

During this section, we will work with three practical operation examples, whose load signals were acquired, and will be used to show the problems and test the developed solutions. The first example signal, which will be named signal **A** and can be seen in Figure 5, was acquired with a low SNR ratio. The second example signal, which will be named signal **B** and can be seen in Figure 6, was acquired with a low SNR ratio, high idle load and a temperature drift in the sensor. The third example signal, which will be named signal **C** and can be seen in Figure 7, was acquired with a good SNR ratio, and practically no idle load, which will therefore be used as a benchmark.

Low pass filter

To find an appropriate low pass filter, the student evaluated qualitatively some IIR filters and FIR filters based on implementation and tuning complexity, falloff after cutoff frequency, computational complexity, step/impulse response performance and potential for improvement. All filters were tested with minimal tuning, to better test tuning time and complexity. The filters to be tested were chosen by finding commonly used filters in popular signal processing libraries for Python, such as scipy (SCIPY, 2023) and pandas (PANDAS, 2023). All filters tested were tuned to have a cutoff frequency of around 2 Hz, as this passing band was qualitatively found to contain the highest amount of useful information about the milling process. We will first go over the IIR filters, as they are the most commonly used in the Control and Automation Engineering course.

IIR filters

The filters to be tested are a lowpass Butterworth filter, which is known for having the flattest possible pass band, and a low pass Chebyshev type I filter, which has a faster roll off than Butterworth filters, but have ripples in the pass band. This can be seen in Figure 8. IIR filters are usually very simple to implement, tune and compute, but can not be improved much further.

Figure 8 – Frequency response of the tested IIR filters.

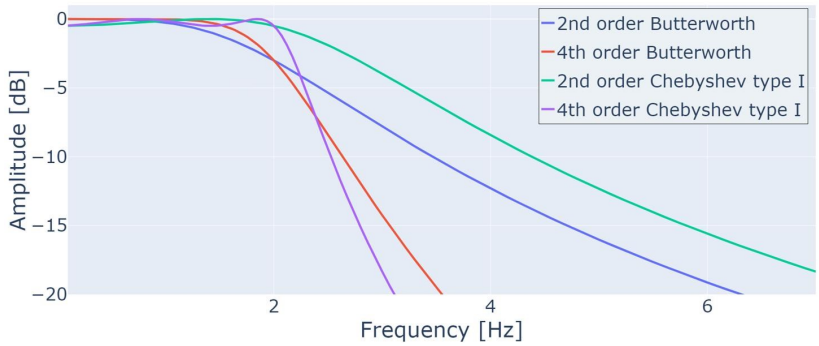

Source: student's archive.

Comparing their impulse and step response, which can be seen in Figure 9 and Figure 10, the Chebyshev filters have greater oscillation and overshoot than the Butterworth filters. The filters of higher order have better frequency cutoff, but also more oscillations than their lower order counterparts.

Figure 9 – Impulse response of the tested IIR filters.

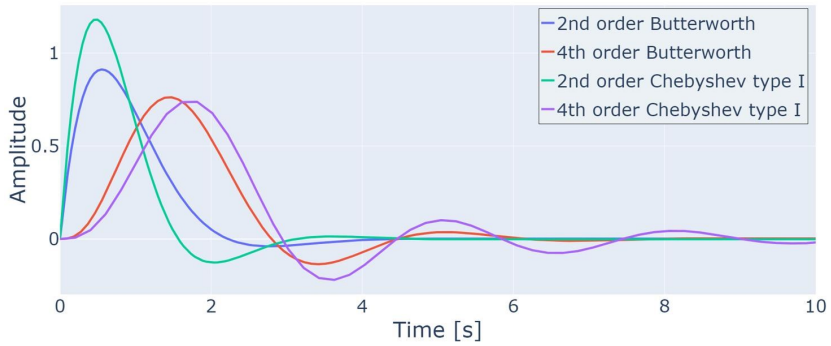

Source: student's archive.

Figure 10 – Step response of the tested IIR filters.

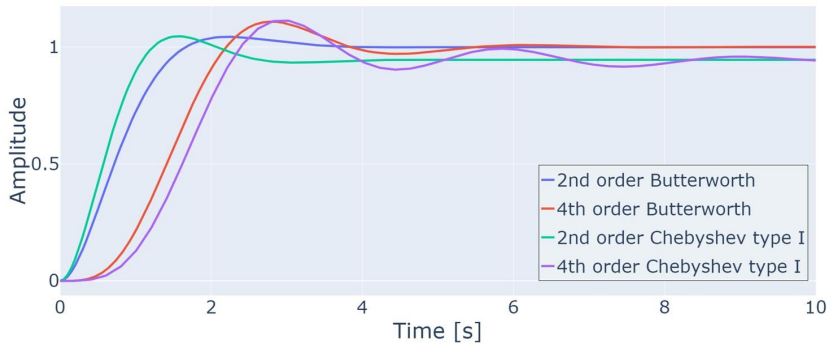

Source: student's archive.

The result of applying these filters on the example signal **A** can be seen in Figure 11 and zoomed in on a feature in Figure 12. The filters were applied twice, once forward and once backward in time, resulting in zero phase offset and doubled attenuation. In this practical example, it's noticeable that 2nd order filters do not have a fast enough roll off to properly filter some of the higher frequency noise present in the signal. We can then discard them from further testing.

Figure 11 – Response of the IIR filters applied on example **A**.

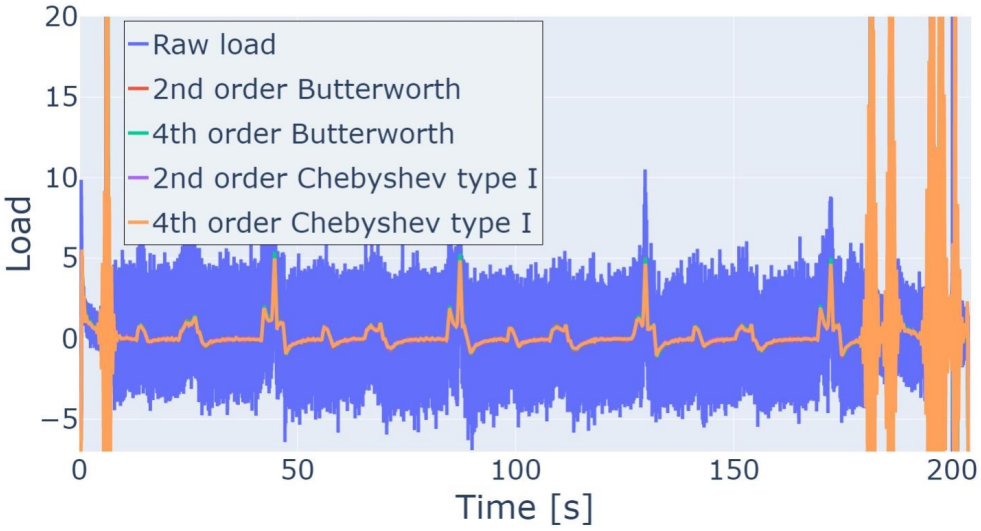

Source: student's archive.

Figure 12 – Response of the IIR filters applied on example **A**. Zoomed in on a feature to better analyze filter performance.

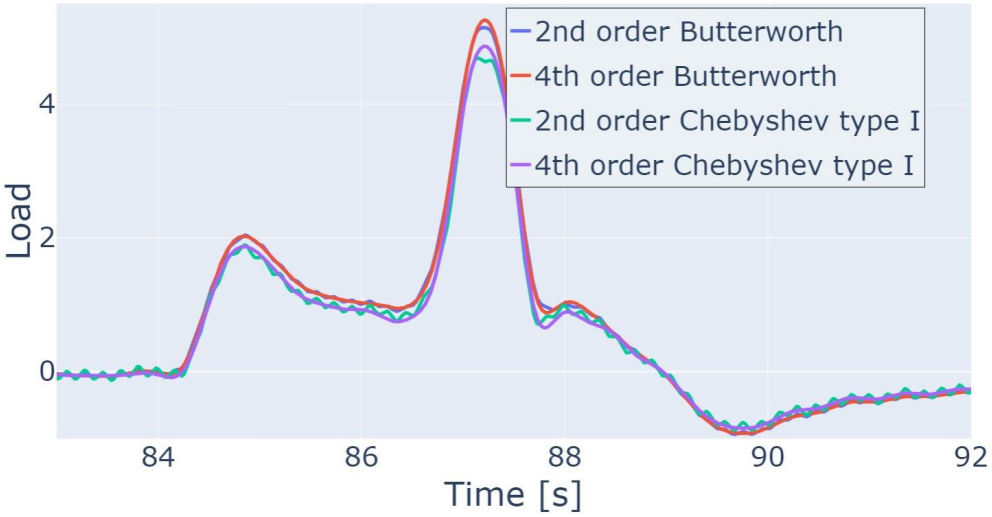

Source: student's archive.

FIR filters

The window functions to be tested are the Boxcar window (1) (moving average), Hann window (2), Blackman window (3), Blackman-Harris window (4) and Blackman–Nuttall window (5). The window size was chosen to be the acquisition frequency f_s divided by the desired cutoff frequency f_c, as an approximated way of choosing their actual cutoff frequency. As a note, the Boxcar window was tested only as a demonstration of a simple FIR filter, and how its performance can change given the chosen

window design. FIR filters are usually harder to implement and design, and more computationally expensive than IIR filters, but can be fine tuned to a much bigger extent, giving more control of their filtering performance.

The frequency response of these filters can be seen in Figure 13. The Blackman-Harris and Blackman-Nutall windows have stronger higher frequency attenuation, but slower initial roll off. The Boxcar and Hann window have a faster initial roll off, but weaker high frequency attenuation, and the Blackman window seems to strike a good balance in these regards.

Figure 13 – Frequency response of the tested FIR filters.

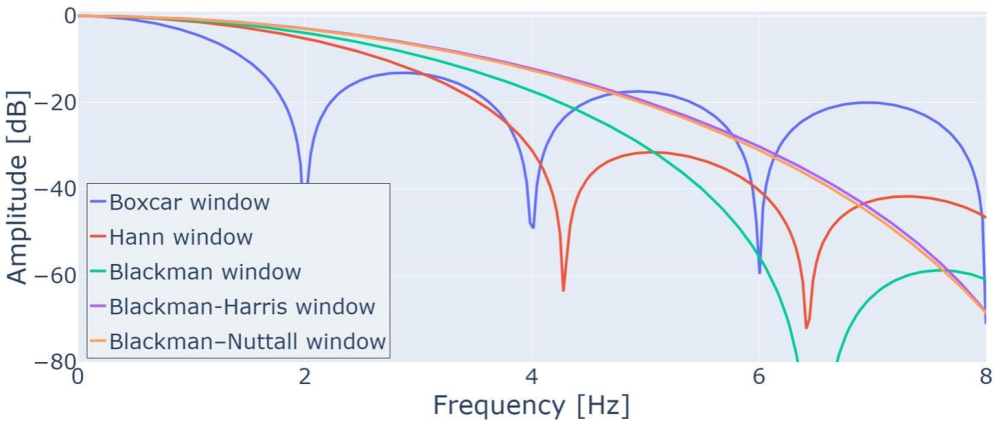

Source: student's archive.

The unit impulse and unit step response performance of FIR filters are significantly better than the response of the IIR filters, with no oscillations, ringing or overshoot. It is interesting to note that the impulse response of the FIR filters is simply the window function, and that their response is finite, thus their name.

Figure 14 – Unit impulse response of the tested FIR filters.

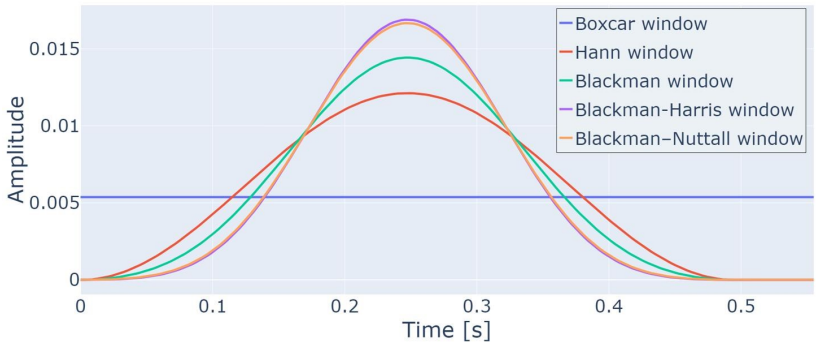

Source: student's archive.

Figure 15 – Unit step response of the tested FIR filters.

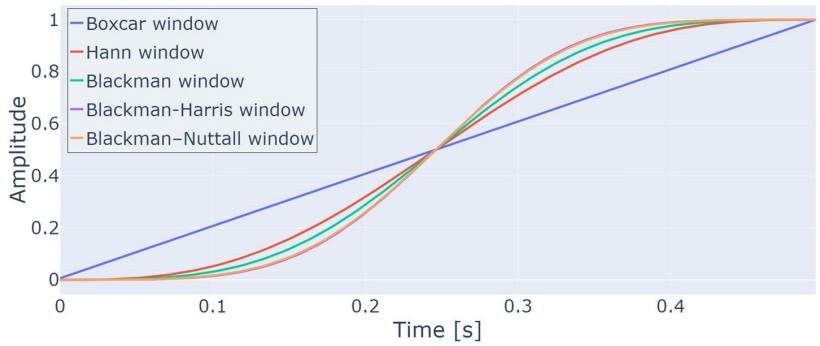

Source: student's archive.

The result of applying these filters on the example signal **A** can be seen zoomed in on a feature in Figure 16. The filters were applied using a centralized convolution, as to result in zero phase offset. All the filters present very good performance, other than the Boxcar filter. Upon closer inspection of the remaining filters, given this quick tuning, the student selected the Hann window and Blackman window for further testing (Figure 17), as their faster roll off made a more significant difference, compared with the Blackman-Harris and Blackman-Nuttall windows, given that the higher frequencies were strongly attenuated by all four of them.

Figure 16 – Response of the FIR filters applied on example **A**. Zoomed in on a feature to better analyze filter performance.

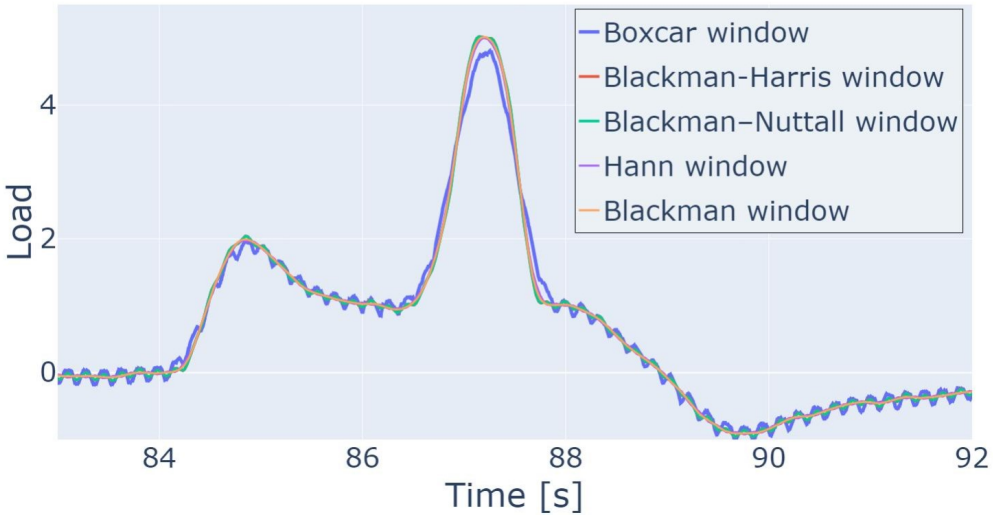

Source: student's archive.

Figure 17 – Response of the FIR filters applied on example **A**. Zoomed in on a feature to better analyze filter performance, with only the filters chosen by the student for further testing.

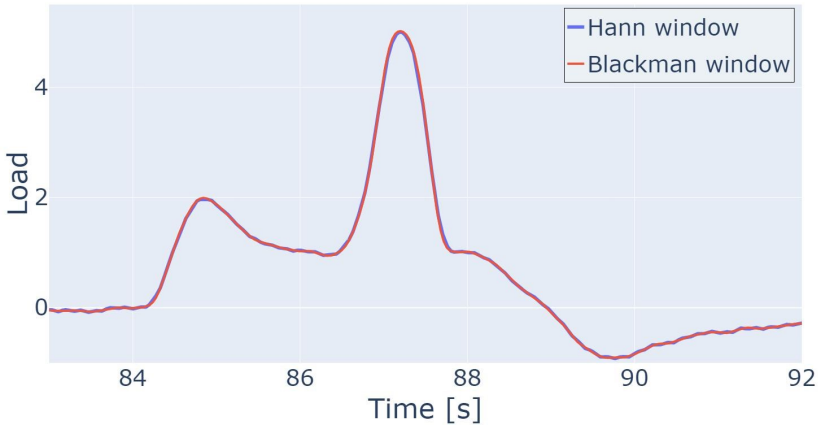

Source: student's archive.

Finally, a comparison between the chosen FIR filters and IIR filters can be seen in Figure 18 and Figure 19. The student then created a table, Table 2, qualitatively evaluating the performance of the chosen filters in the previously mentioned aspects with a - sign for bad or unsatisfactory, nothing for reasonable or unremarkable, and a + sign for good or satisfactory.

Table 2 – Qualitative evaluation of low pass filter performance. **A** - Difficulty of implementation and tuning complexity, **B** - Frequency roll off, **C** - High frequency attenuation, **D** - Computational complexity, **E** - Step/impulse response, **F** - Possibility of improvement.

Type	Name	A	B	C	D	E	F	TOTAL
IIR	Butterworth	+			+	-	-	0
	Chebyshev		+	+	+	-		2
FIR	Boxcar	+	-	-	+	-	-	-2
	Hann	+	+			+		3
	Blackman	+	+	+		+		4
	Blackman-Harris			+		+	+	3
	Blackman-Nuttall			+		+	+	3

Source: student's archive.

Figure 18 – Response of the chosen FIR and IIR filters applied on example **A**.

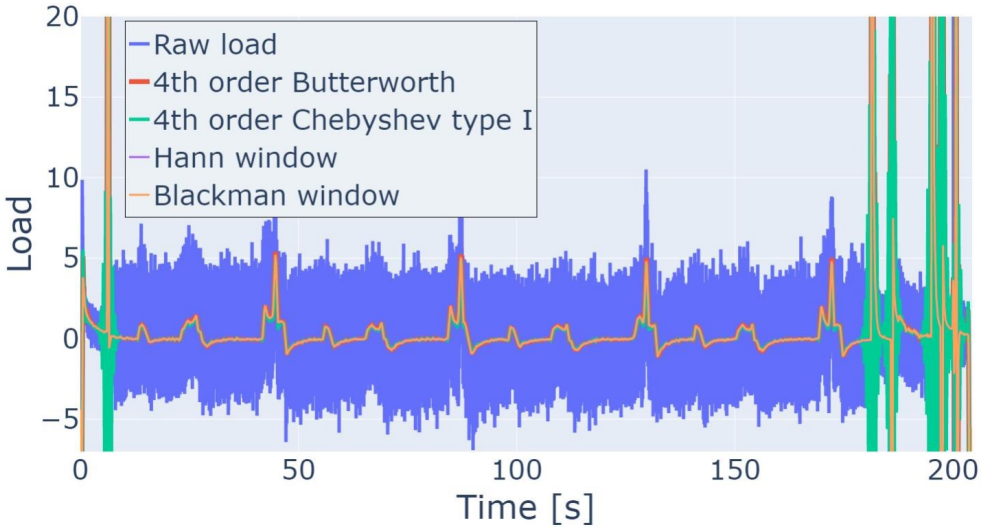

Source: student's archive.

Figure 19 – Response of the chosen FIR and IIR filters applied on example **A**. Zoomed in on a feature to better analyze filter performance.

Source: student's archive.

Figure 20 – Response of the chosen FIR and IIR filters applied on example **B**.

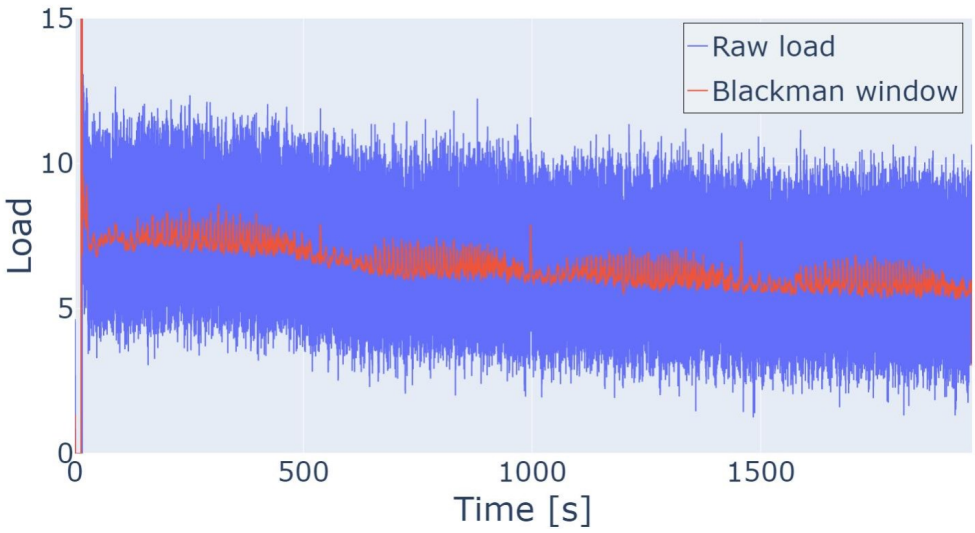

Source: student's archive.

Figure 21 – Response of the chosen FIR and IIR filters applied on example **C**.

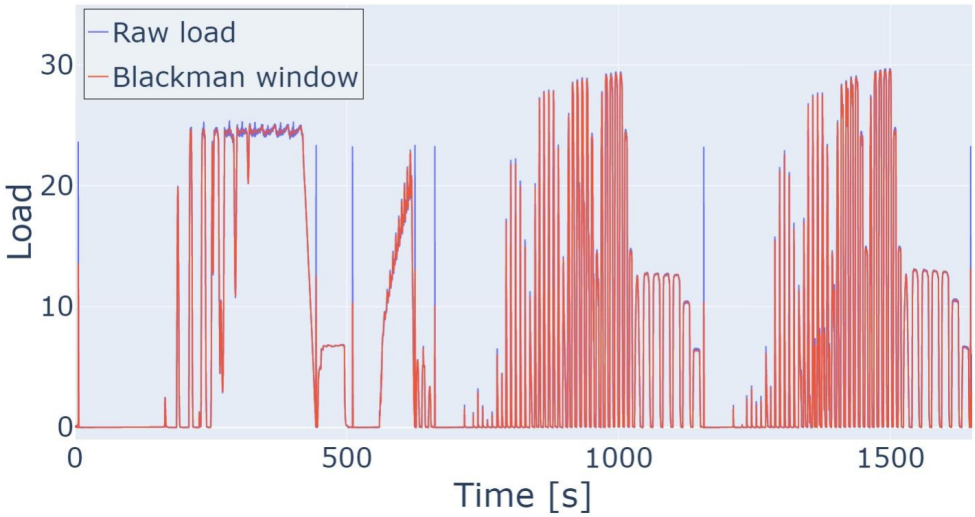

Source: student's archive.

With the use of this table, the student decided to implement the Blackman window as a FIR low pass filter for the load signal. The performance of the chosen filter was found satisfactory, leading to its implementation into the service.

4 FORCE MODELING

This chapter describes the process used by the student in finding an approximation for the rotational load of a milling tool for a given tool move. It describes the analytical and numerical process for the generation of new simulation and force prediction data from the engagement output, based on industry standard models of milling forces.

The approach for approximating the process forces used in this chapter is similar to the approach used by (ALTINTAS; LEE, 1998) for applying his force model numerically.

CUTTING EDGE CONTACT SIMULATION

In order to test the method developed by the student, simulations were performed with the same milling parameters as the tests performed by Cabral (2015) in his PhD thesis. In his work, he used a much more thorough simulation of the forces in a milling process, taking into account many more variables regarding the tool micro geometry, and thus should be regarded as more accurate than this work's approach, which is meant as a fast approximation of the force profile. With that said, the results of the experiments performed with the student's framework show many of the same behaviors regarding changing technological parameters, with satisfactory accuracy in the predictions for the given use case. The default parameters used for the simulation, done with a ball end mill geometry, can be seen in Table 3.

The result of the simulations with varying technological parameters can be seen in Figure 24 with changing f_z, Figure 25 with changing depth of cut, Figure 26 with changing step over, Figure 27 with changing helix angle and Figure 28 with changing tool radius. For better visualization of the technological parameters used in these experiments, the 3D engagement region can be seen in Figure 22 with a helix angle of 40°, as well as the tool engaged with the workpiece geometry, and a closer view of the resulting machined workpiece.

Table 3 – Default simulation parameters used for the comparison with Cabral (2015).

Parameter	Symbol	Value
Tool radius	R_0	3 mm
Tool helix angle	λ	10°
Step over	a_e	0.1 mm
Depth of cut	a_p	0.1 mm
Feed per tooth	f_z	0.03 mm

Source: Personal archive

Figure 22 – Visualization in 3D of the cutting tool and workpiece used for the comparison with Cabral's work: A ball end mill of radius 3 mm and helix angle 40°. From left to right, the cutting tool engaged with the workpiece, the cutting tool with the engagement region and the cutting edge geometry highlighted, and the resulting cut workpiece at the moment of measurement.

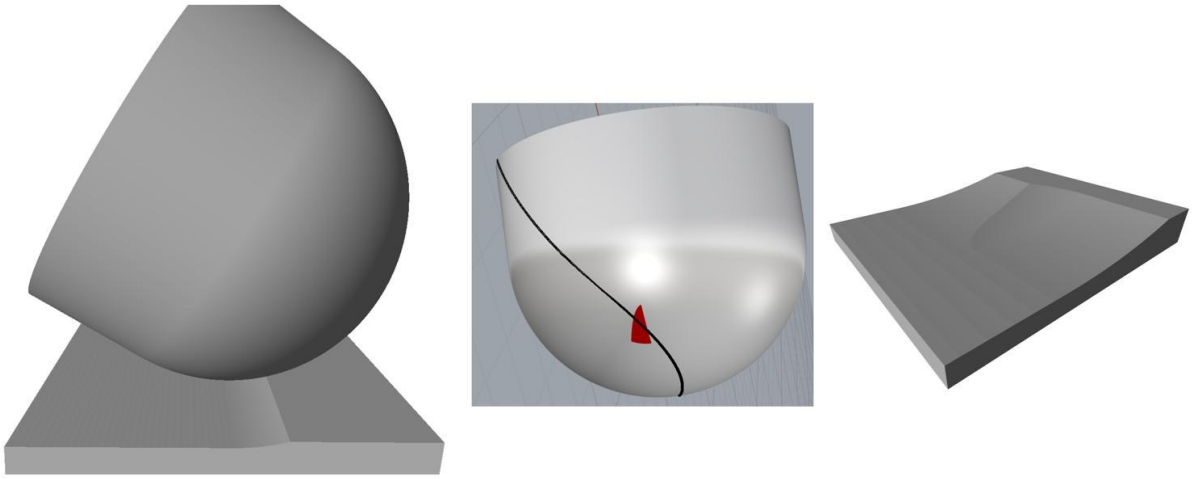

Source: Personal archive.

Figure 23 – This figure draws a parallel of the engaged region in 2D with their corresponding positions in the 3D engagement surface. The green line is the edge of the engaged region restricted by the not yet cut surface of the workpiece.

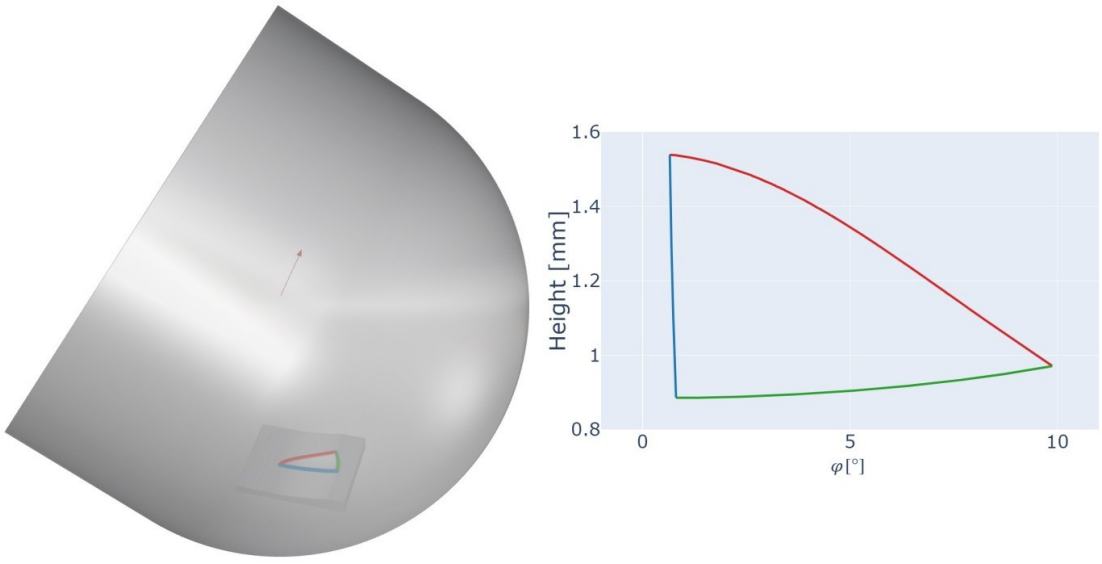

Source: Personal archive.

In order to facilitate the understanding of how the engagement surface changes with the variations in the technological parameters, Figure 40 presents where the limits of the engagement surface are located in the 3D cut, and how it matches to the 2D engagement surface. The green line represents the engagement surface that is restricted by the uncut region of the workpiece, the red line represents the restriction made by

previous cuts with the same tool and the blue line represents the restriction made by the cross section of the cutting tool. For the rest of this section, these curve sections are referenced by their respective colors in Figure 40.

Figure 24 – Simulated parameters of the force profile calculation and their behavior with changing feed per tooth.

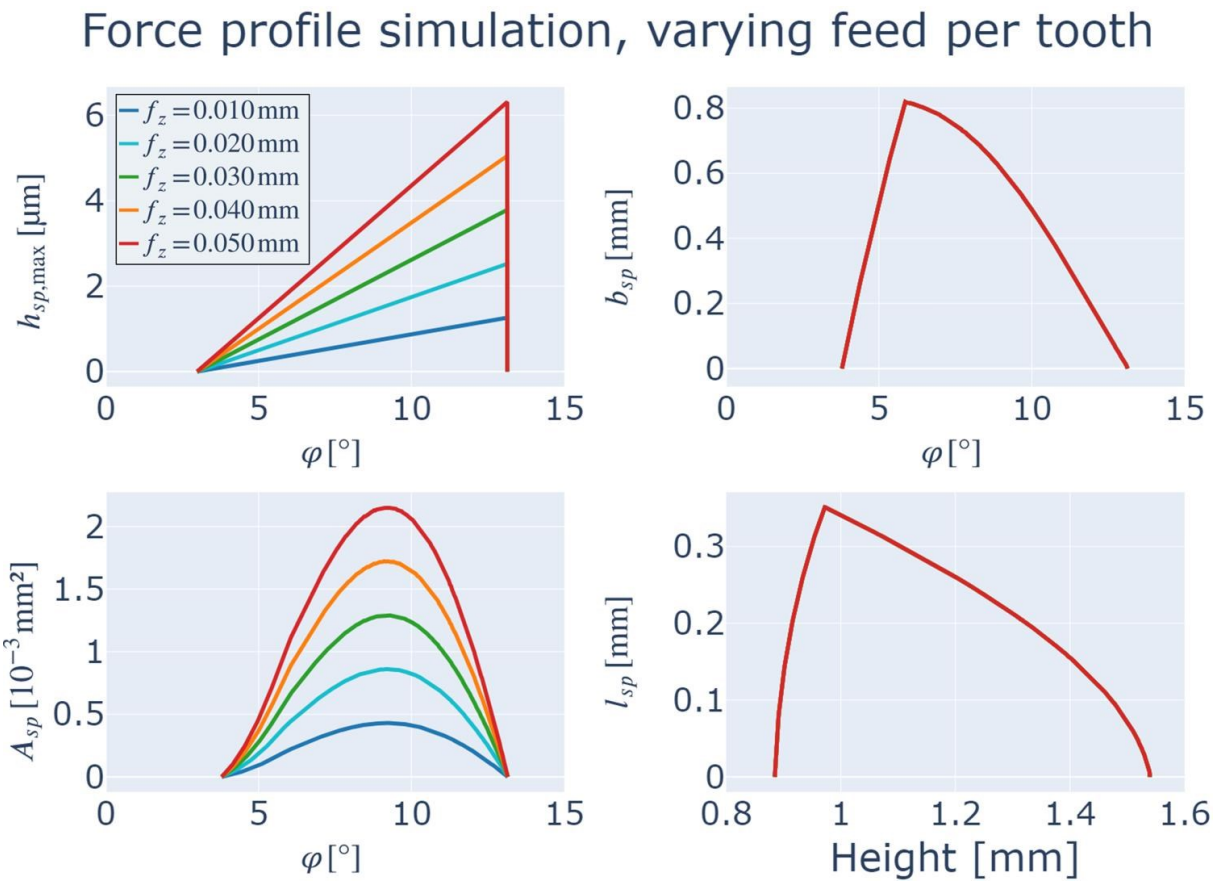

Source: Personal archive.

Figure 24 presents how the uncut chip parameters behave when the feed per tooth f_z of the cut changes. The chip thickness h_{sp} depends linearly on f_z, thus we can see it increase as f_z increases. In the developed contact edge simulation, the engaged region does not change with f_z, and as such, both the chip length l_{sp} and chip width b_{sp} are constant. As the chip cross sectional area depends on both b_{sp} and h_{sp}, it also increases with an increase on f_z. We can then infer that an increase in f_z will approximately linearly increase the force without changes in its acting direction. The acting direction of the force is given roughly by the relative distance of the A_{sp} peak to the start of the signal, in other words, where the peak is located within the engaged region.

It is important to note that increasing the feedrate v_f increases f_z, and increasing the spindle speed decreases f_z.

Figure 25 – Simulated parameters of the force profile calculation and their behavior with changing depth of cut.

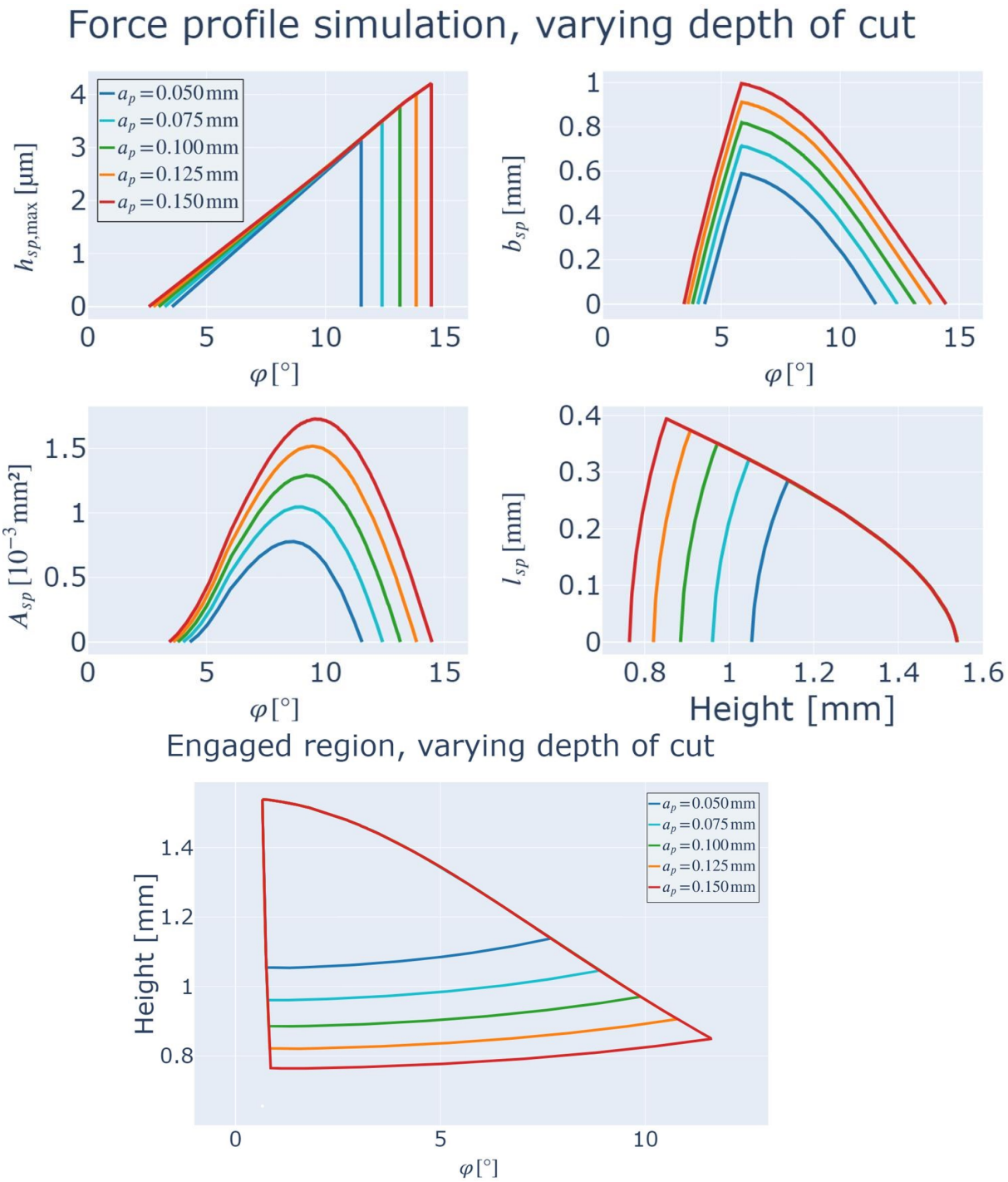

Source: Personal archive.

Figure 25 presents how the uncut chip parameters behave with changing depth of cut a_p. As the distance between consecutive cuts remains constant, the shape of the blue and red engagement limits remains the same, only getting longer as the tool is cutting deeper into material. As the engagement region grows, the b_{sp} and l_{sp} grow in height and width. As the engagement region also extends towards the movement direction of the cut, A_{sp} and h_{sp} both grow as their peaks move also towards the

movement direction. From this we can infer that the cutting forces grow with increases of a_p, as well as its acting direction moving closer to the opposite the cutting tool movement.

Figure 26 – Simulated parameters of the force profile calculation and their behavior with changing step over.

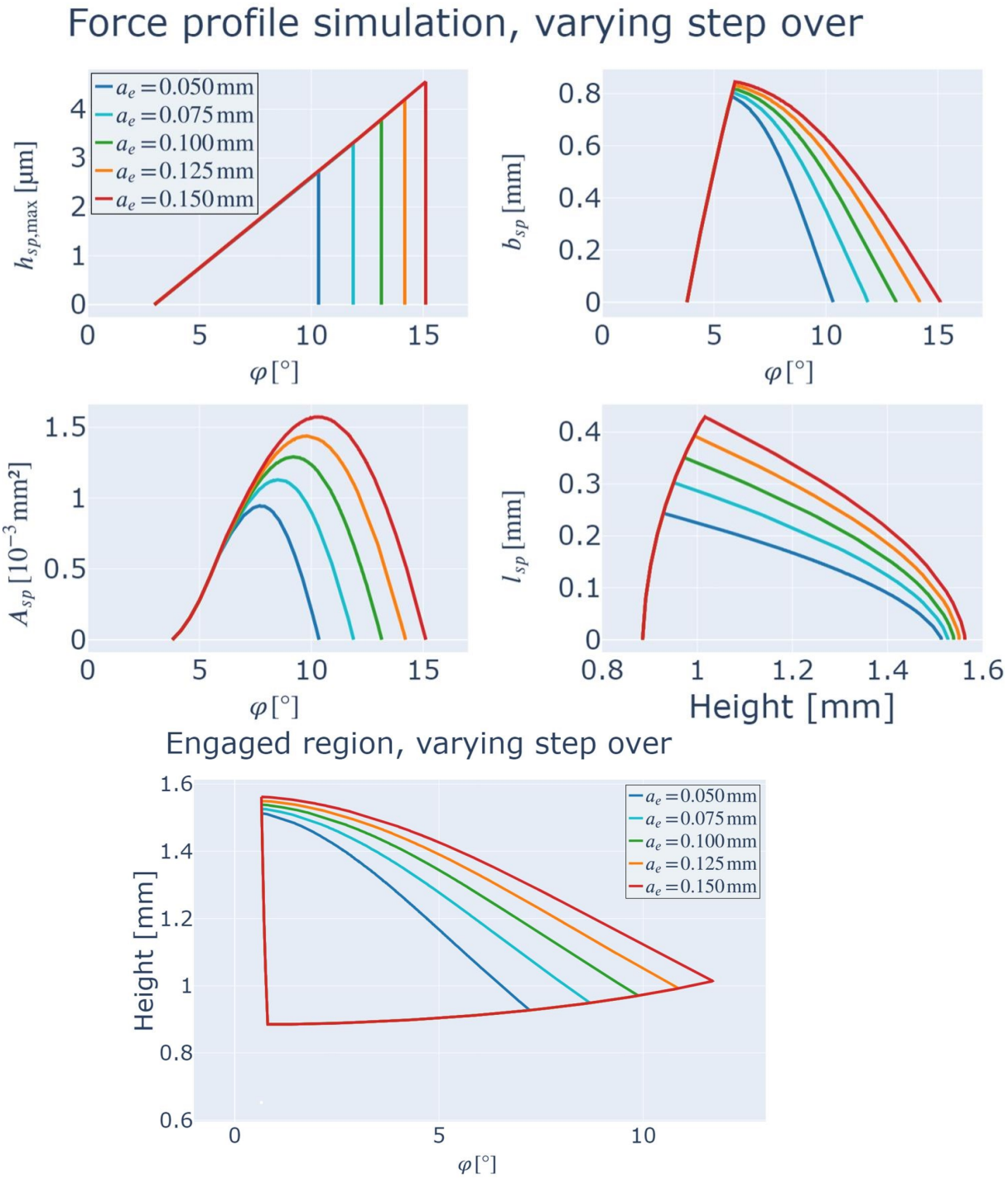

Source: Personal archive.

With changing step over a_e, the red engagement limit curve changes as the length of the uncut workpiece that is cut by then tool gets longer, as can be seen in

Figure 26. As the uncut chip surface grows towards the movement direction, again the h_{sp} grows wider and taller. The b_{sp} however, grows much faster in width than in height, as the engaged region gets wider more rapidly than it grows taller. The same explains the height growth in l_{sp}. In consequence to the direction of the growth in b_{sp} and h_{sp}, A_{sp} grows rapidly in height with its peak moving toward the direction of movement. Given this analysis, we can infer that the acting direction of the cutting forces shifts rapidly towards the movement direction of the cutting tool with increases in step over, as well as increasing also in magnitude.

Figure 27 – Simulated parameters of the force profile calculation and their behavior with changing tool helix angle.

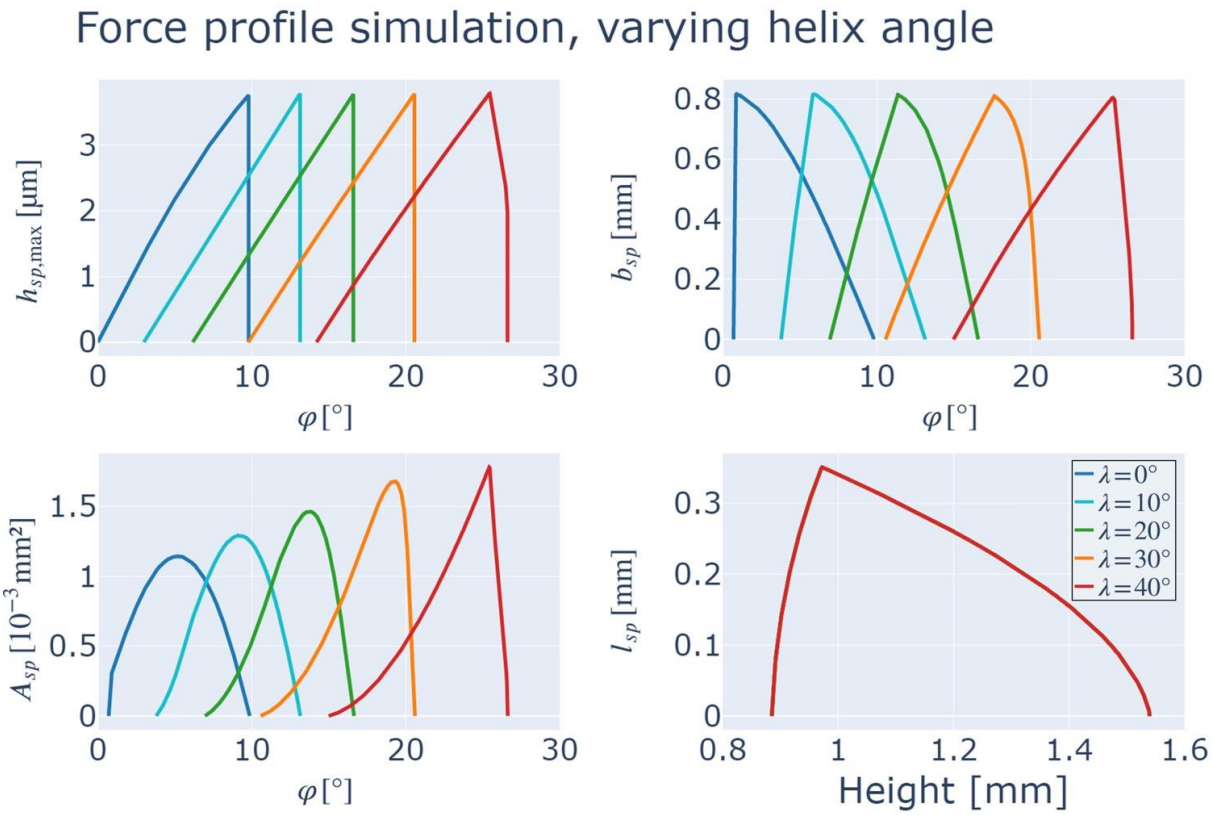

Source: Personal archive.

Variations in the cutting teeth helix angle λ do not affect the engagement region, it does however change its position relative to the cutting edges angular position, as can be seen by shift position shift of the uncut chip parameters in Figure 27. Said figure also shows how λ has a strong effect on the behavior of the b_{sp}. As in addition the angular shift, its speed of growth and decay change sharply as the alignment of the cutting edge interacts with the engagement surface, and its peak value decreases slightly. With increasing λ h_{sp} gets slightly wider, and A_{sp} gets taller and sharper, and it its peak moves closer to the movement direction. We can infer from this, that the cutting forces increase and shift their acting direction towards the movement direction as λ increases.

Figure 28 – Simulated parameters of the force profile calculation and their behavior with changing tool radius.

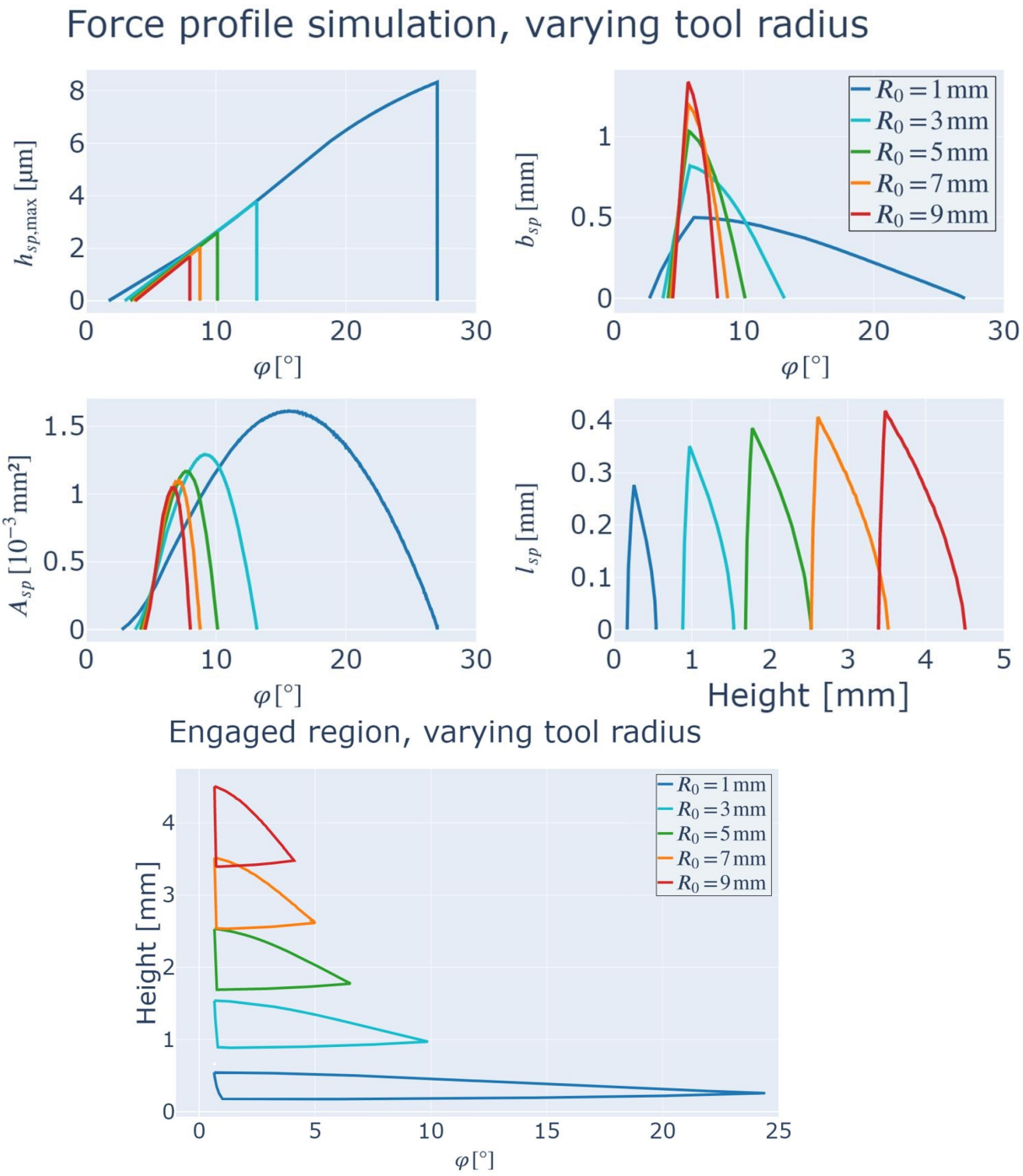

Source: Personal archive.

Figure 28 shows how big of an effect the cutting tool nominal radius R_0 has on the shape of the uncut chip geometry. We can see that as R_0 increases, the width of the engagement region decreases very rapidly, even though the chip length l_{sp} actually increases, showing that the tool's perimeter grows much faster than the increased contact surface. As it can be noted in the l_{sp} graph, the contact surface growth is apparently logarithmic. Consequently, as the cutting speed $\frac{1}{60}\omega.R_0$ of the cutting tool

increases linearly with its radius, the time taken to cut the chip gets shorter, as seen in the remaining uncut chip parameters getting more concentrated and shifting further away from the movement direction, for a constant ω. Because of these reasons, the h_{sp} decreases, and the b_{sp} increases, as both get concentrated and the surface area grows, while A_{sp} decreases.

We can then infer that, for an increasing R_0, the cutting forces get shorter and more concentrated in time, and can either increase or decrease, depending on the ratio between the cutting coefficient and the edge coefficient, as the b_{sp} and A_{sp} have opposite behaviors for changes in R_0.

Table 4 summarizes the previous analysis, presenting how the changes in technological parameters affects the uncut chip geometry for the studied cut. It is important to note that these relationships are not general, and can change for different tool orientations in relation to the workpiece surface, and for different cutting tool geometries.

Table 4 – Summary of how the uncut chip geometry behaves in response to increases in the technological parameters of the studied milling operation .

	f_z	a_p	a_e	λ	R_0
$h_{sp,\,max}$	↑	↑	↑		↓
b_{sp}		↑	↑	↓	↑
l_{sp}		↑	↑		↑
A_{sp}	↑	↑	↑	↑	↓
Cutting time		↑	↑	↑	↓

Source: Personal archive

5 EXPERIMENTAL RESULTS

This chapter will present the experimental results from tests performed using the methods previously developed, resenting a small selection of digital twins, highlighting the deviation differences between the simulated nominal toolpath, and the deflected toolpath.

5.1 DEVIATION COMPARISON

To demonstrate the effects of the tool deflection, an example process was chosen that contained simple cuts using an end mill of diameter 25 mm. The nominal geometry of this workpiece can be seen in Figure 29. After the workpiece was milled and its data was acquired, the simulation of the nominal toolpath was performed. The resulting workpiece was then colored by its deviation from the nominal geometry, and can be seen together with its color scale in Figure 30. The toolpath and the cutting tool at the
middle of the highlighted region can be seen in Figure 31, the toolpath is colored by the A_{surf} with the interval [0, 273] mm^2.

Figure 29 – Nominal geometry of the digital twin, whose operations are simple cuts. The highlighted right wall of the geometry was roughly measured after the milling process, it had a deviation of around 0.1 mm.

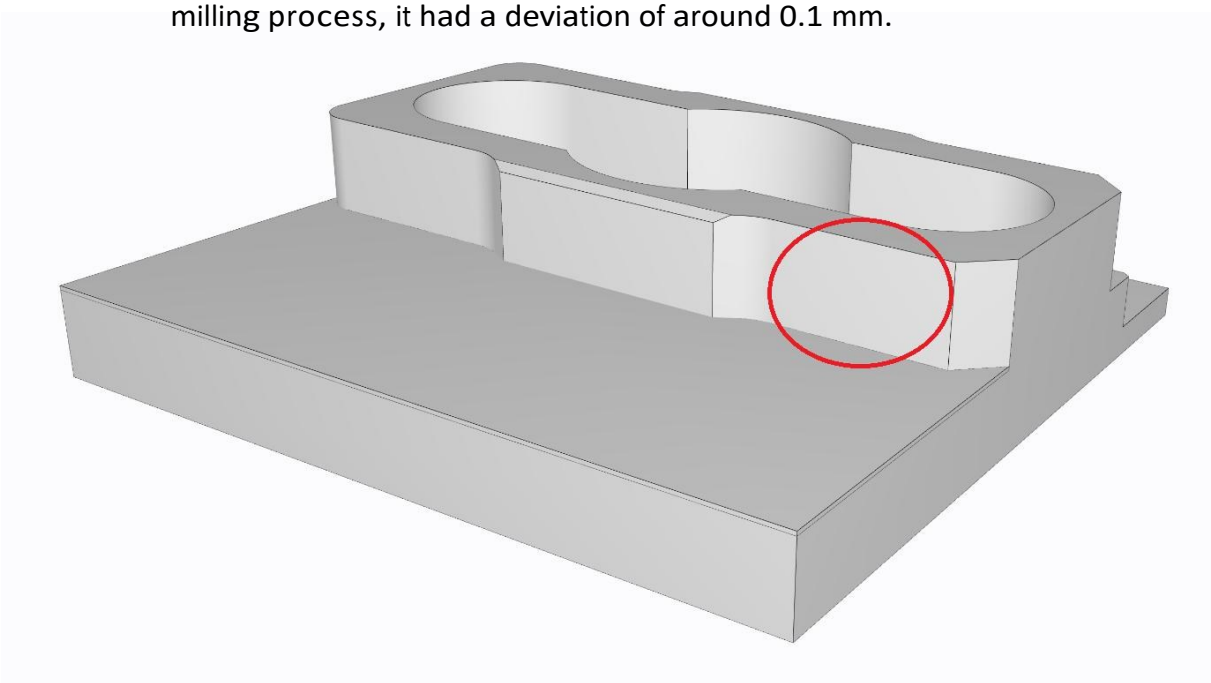

Source: Personal archive.

Figure 30 – Result of the cutting simulation using the nominal toolpath, colored by the deviation from the nominal geometry.

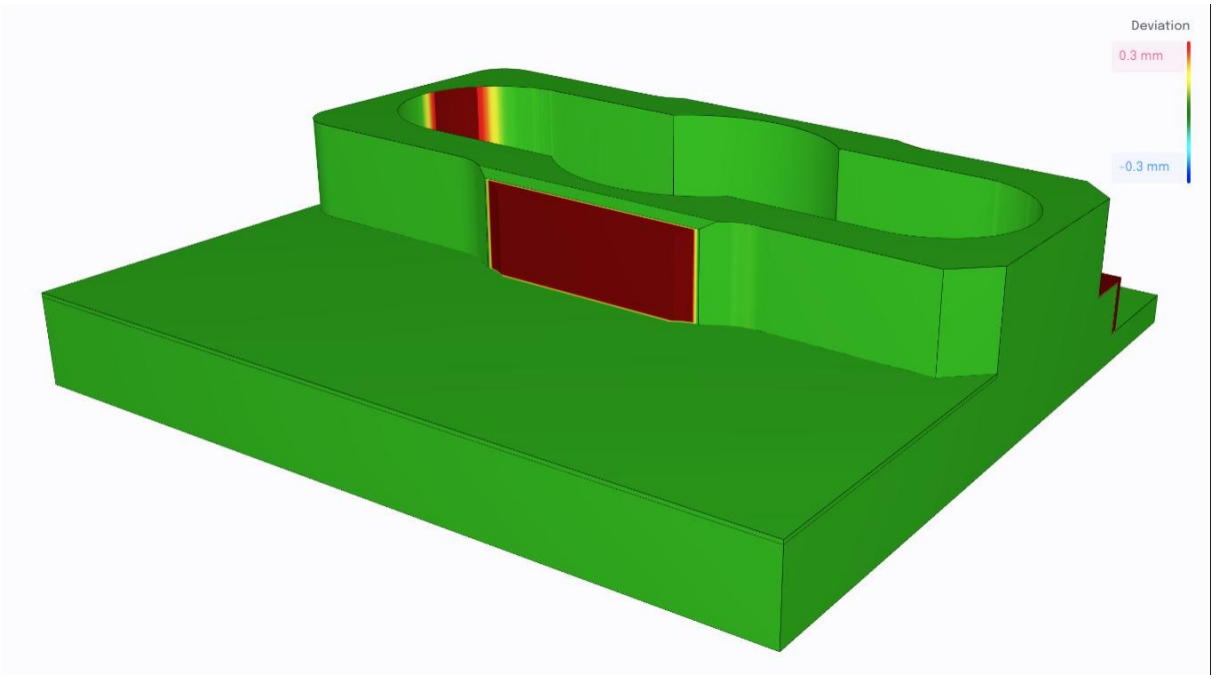

Source: Personal archive.

Figure 31 – Visulization of the cutting tool removing material from the workpiece in the region of interest. The workpiece is colored by its deviation from the nominal geometry, and the toolpath is colored by A_{surf} with the interval [0, 273] mm^2.

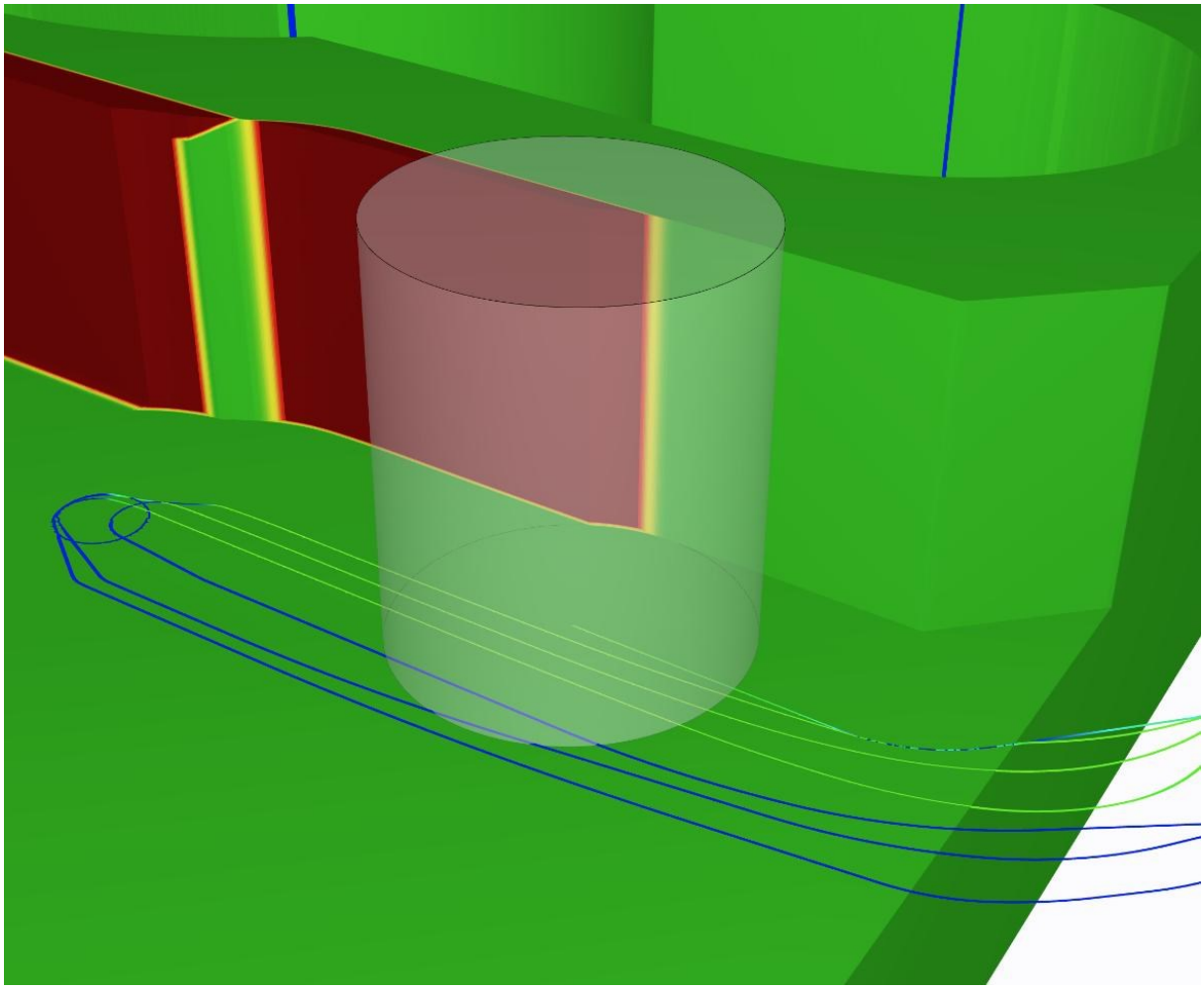

Source: Personal archive.

Applying the algorithms developed in this work and in the internship project, the resulting simulation data is then used to calculate a force prediction, and apply this force on the cutting tool, deflecting its toolpath. By simulating then this deflected toolpath, the result in Figure 32 is achieved, with a deviation of 0.15 mm in the region of interest.

Figure 32 – Result of the cutting simulation using the deflected toolpath, colored by the deviation from the nominal geometry.

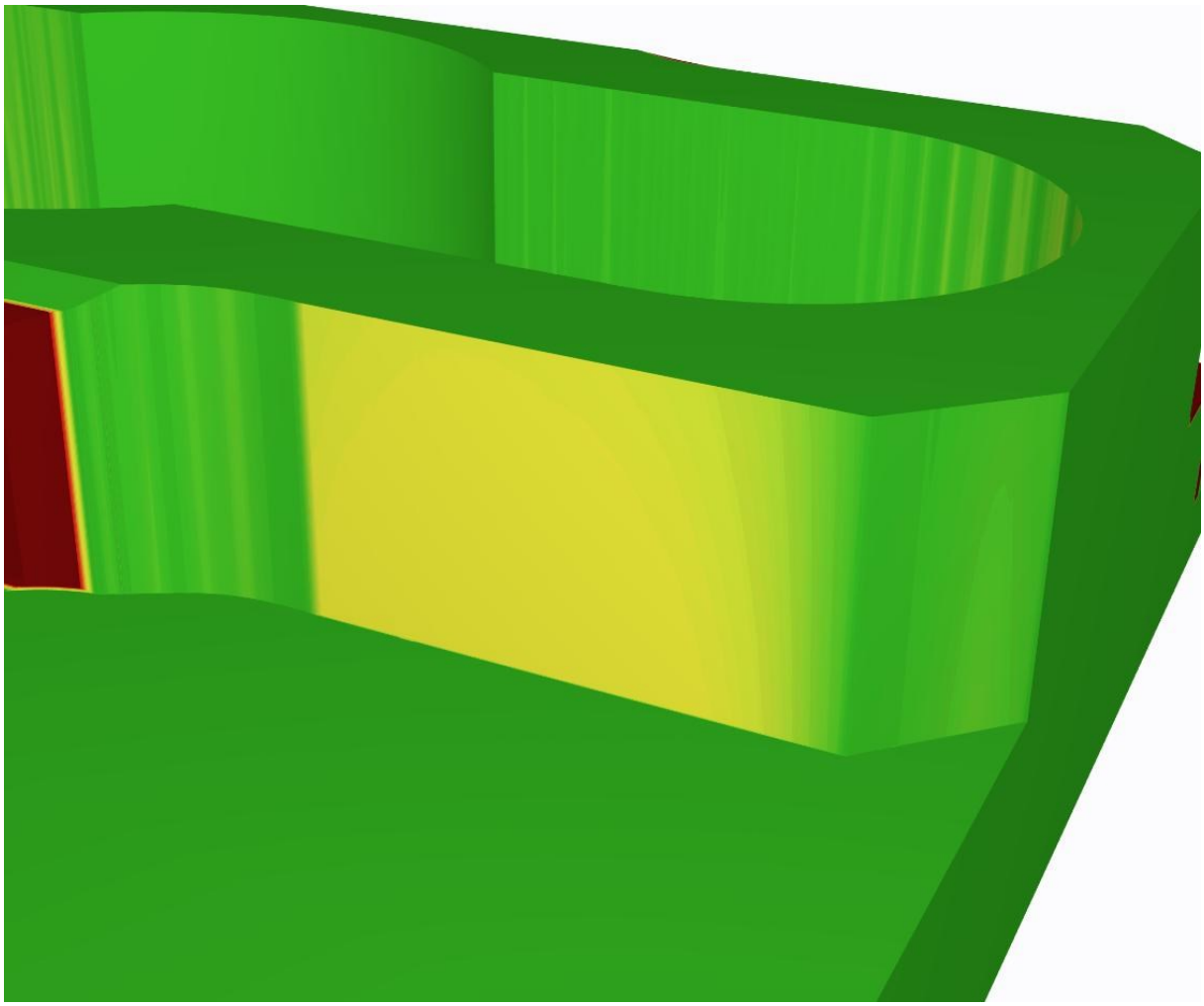

Source: Personal archive.

After this workpiece was milled, a second one was processed with slightly different technological parameters, which then caused the cutting tool to experience stronger forces. The same cutting tools and initial geometry were used for the making and simulation of this second part. The simulation result using the data acquired from this second workpiece can be seen in Figure 33, where the deviations in the lower part of the region of interest are in the neighborhood of 0.24 mm. The measurements performed on the same region in the machined workpiece range around 0.28 mm.

Figure 33 – Result of the cutting simulation using the deflected toolpath of the second machined part, colored by the deviation from the nominal geometry.

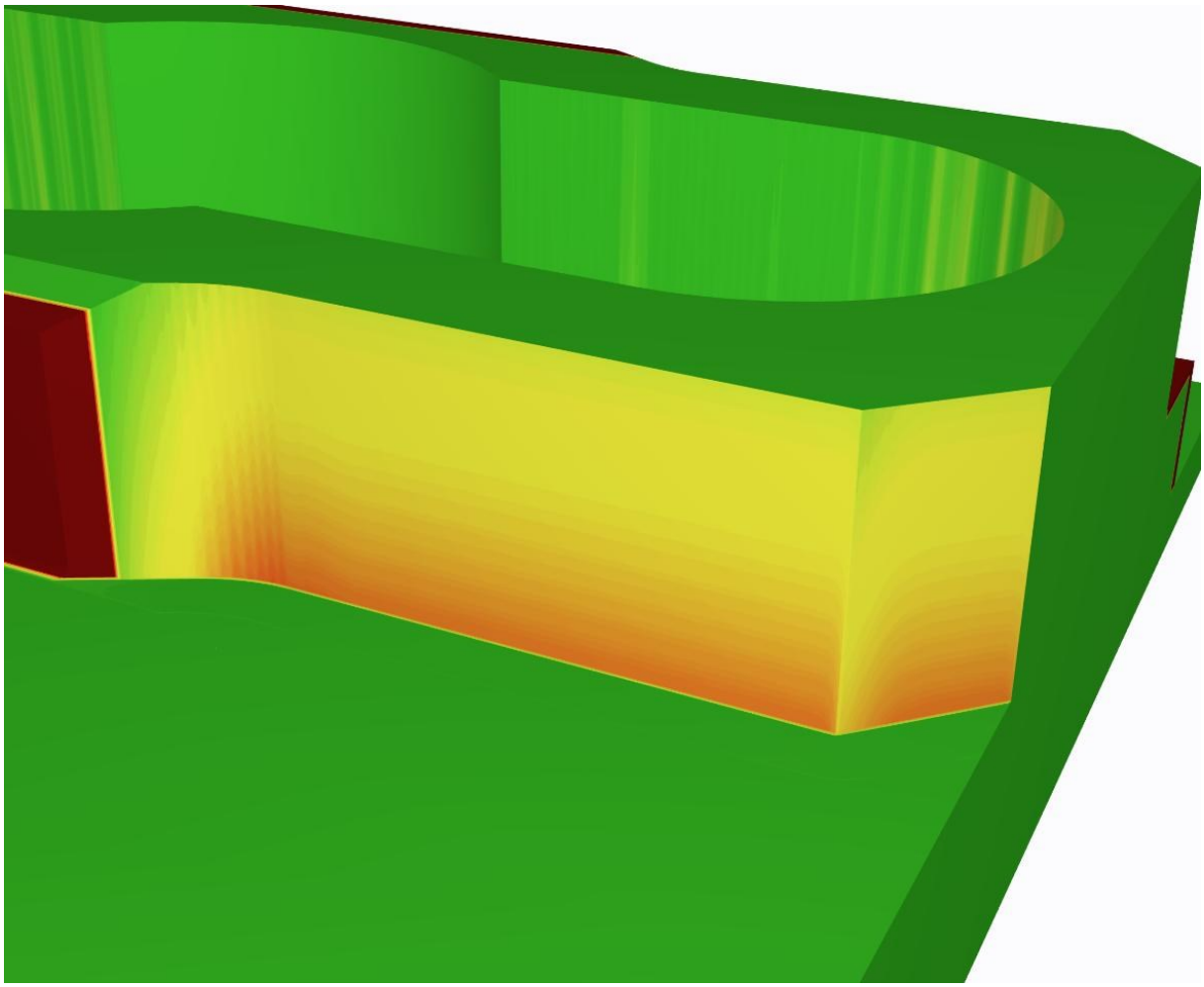

Source: Personal archive.

A second example nominal geometry can be seen in Figure 34, with a region that was studied highlighted in red, as well as the deviation colored geometry in the second picture. The color interval in the second picture is [-0.1, 0.1] mm, and the deviations in this geometry are mainly due to errors in the signal acquisition and in the nominal toolpath. The cuts performed in this workpiece were much more complex than the ones from the previous example, this is the source of the studied signal of the example **A** in Figure 5.

Figure 34 – Nominal geometry of the second digital twin. The deviations of the highlighted part were chosen to be studied due to it being caused by simple cuts with a clear load signal. The second picture is colored by its deviation after being cut with the nominal toolpath, the deviations shown are due mainly to acquisition errors and toolpath errors. The color scale is [-0.1, 0.1] mm.

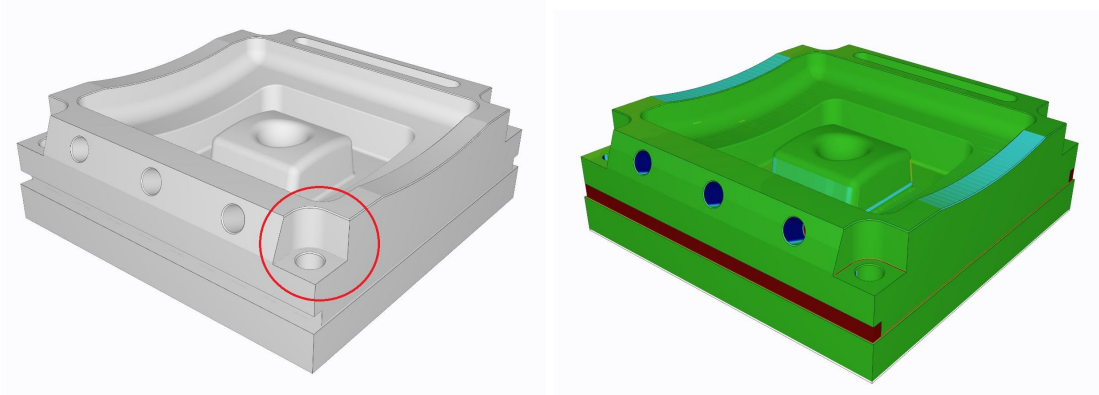

Source: Personal archive.

Figure 35 presents a closer view of the deviation geometry on the highlighted feature, while Figure 36 shows the result of the simulation of the deflected toolpath, with a color scale of [-0.1, 0.1] mm in the first picture, and a color scale of [-0.2, 0.2] mm in the second picture.

Figure 35 – Result of the cutting simulation using the nominal toolpath, colored by the deviation from the nominal geometry. Closer view of the selected feature.

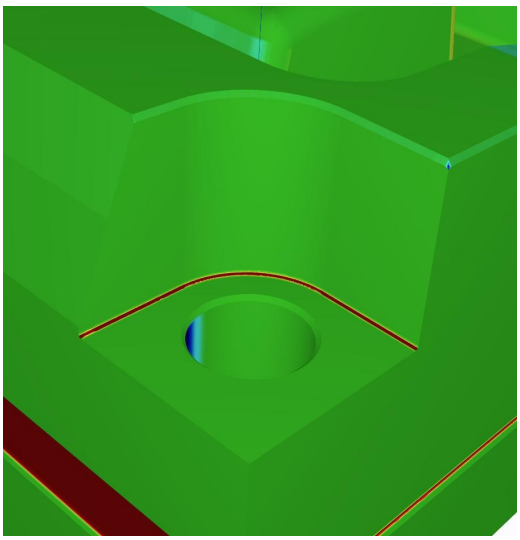

Source: Personal archive.

Figure 36 – Result of the cutting simulation using the deflected toolpath, colored by the deviation from the nominal geometry. Closer view of the selected feature. Color scale of [-0.1, 0.1] mm in the first picture, and a color scale of [-0.2, 0.2] mm in the second picture

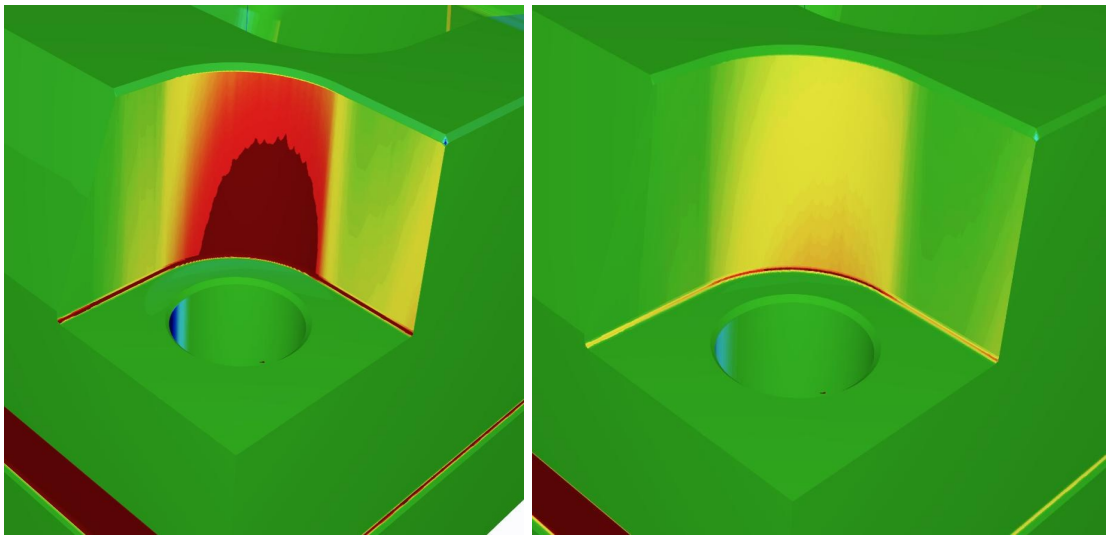

Source: Personal archive.

The tests performed in this chapter, due to time constraints, to the costs of running a milling machine tool, and the scarce machine availability in the **company** for undergraduate testing purposes, were not particularly rigorous. The data used and presented were acquired from client projects, in real industry machining applications, where measurements and system identifications had to be done in a fast and rough manner. This means that for the simulation, there were uncertainties in the cutting tool and machine information. Nevertheless, the resulting predictions and their accuracy were more than enough for their respective use cases, demonstrating a certain robustness of the software and algorithms developed by the student.

6 CONCLUSION

The objective of this work was to improve the creation of digital twins of the **company** software for milling quality prediction. This was carried out by filtering machine acquired signals from a milling process, performing a cutting simulation using said signals, and then utilizing the filtered signals as well as data resulted from the simulations in order to predict the cutting forces applied by the cutting tool during the milling process.

These predicted cutting forces were then used to calculate the deflection of the cutting tool geometry during cutting, and then its deflection was integrated in the cutting simulation, generating a corrected digital twin geometry that now contains deviations that were previously unmeasured during machining, caused by deflection of the cutting tool. By implementing these deviations in the digital twin generation, the **company** software has the fidelity of its results improved significantly, better reflecting the real counterpart of the gemini geometry.

Without the use of the **company** software, the measurement of these deviations would have to be performed by an expensive machine or a paid professional, in a dull and lengthy process that scales in costs and difficulty with workpiece complexity. The employment of this software can reduce these costs by selecting which regions of the workpiece need measurement, or if it is even needed in the first place. Another important point is that the quality of the prediction does not suffer with increases in complexity, but it is important to note that the simulation time increases with the physical size of the machined workpiece.

PROJECT SUMMARY

The execution of the project was separated into thee main phases. The first phase was a study for creation of a proper filtering process for the acquired load signals. In it, the student evaluated different filtering methods on their effectiveness, ease of implementation, computational complexity and future growth possibility. The tested filtering methods included FIR filters and IIR filters. At the end of the analysis, the student decided to implement a FIR Blackman window filter into the software.

The second phase described the process of developing a force prediction algorithm, whose results results allow a deeper and finer view into the process dynamics, as well as providing a more accurate prediction of force than what is available from the engagement results alone.

The third phase presented the experimental results, validation of the developed algorithms and comparison with measured process data.

RESULTS

The filtering process developed could successfully filter and prepare the machine acquired signals for further processing. Although not perfect, it can generate satisfactory results for a wide range of machine tool manufacturers, signal quality and process conditions, as well as deal with temperature drifts and non zero offsets on acquired signals.

The developed cutting edge contact simulation had surprisingly promising results when compared with similar projects. This opens the opportunity for further studies of force modeling within the software, as well as enabling deeper understanding of the process dynamics by visualizing and calculating the force behavior during cutting.

FUTURE WORK

More work can be done in the force modeling, researching, testing and implementing more precise and more refined models. The software can also benefit much from a more complete data acquisition system.d

REFERENCES

1000ZITATE. **Carl Friedrich Gauß — Zitate**. [S.l.: s.n.], 2022. Available from: https://1000-zitate.de/autor/Carl+Friedrich+Gau%C3%9F/. Visited on: 10 Nov. 2022.

ALTINTAS, Y.; LEE, P. Mechanics and Dynamics of Ball End Milling. **Journal of Manufacturing Science and Engineering**, v. 120, n. 4, p. 684–692, Nov. 1998. ISSN 1087-1357. DOI: 10.1115/1.2830207. eprint: https://asmedigitalcollection.asme.org/manufacturingscience/article-pdf/120/4/684/5931931/684_1.pdf. Available from: https://doi.org/10.1115/1.2830207.

CABRAL, Gustavo Francisco. **Modeling and simulation of tool engagement and prediction of process forces in milling; 1. Auflage**. 2015. 1 online–ressource (viii, 152 seiten) : illustrationen, diagramme. Dissertation – RWTH Aachen University, Aachen. Auch veröffentlicht auf dem Publikationsserver der RWTH Aachen University; Dissertation, RWTH Aachen University, 2015. ISBN 978-3-86359-427-5. Available from: https://publications.rwth-aachen.de/record/658523.

IBM. **What is a digital twin?** [S.l.: s.n.], 2022. Available from: https://www.ibm.com/topics/what-is-a-digital-twin. Visited on: 26 Sept. 2022.

PANDAS. **pandas**. [S.l.: s.n.], 2023. Available from: https://pandas.pydata.org. Visited on: 6 Apr. 2023.

SCIPY. **SciPy**. [S.l.: s.n.], 2023. Available from: https://scipy.org. Visited on: 6 Apr. 2023.

WINDOW FUNCTIONS

All window functions are defined for $n \in [0, N]$, where N is the window size, and 0 everywhere else.

BOXCAR WINDOW

$$w[n] = 1 \tag{1}$$

HANN WINDOW

$$w[n] = \sin^2 \frac{2\pi n}{N} \tag{2}$$

BLACKMAN WINDOW

$$w[n] = \frac{7938}{18608} - \frac{9240}{18608}\cos\frac{2\pi n}{N} + \frac{1430}{18608}\cos\frac{4\pi n}{N} \tag{3}$$

BLACKMAN-HARRIS WINDOW

$$w[n] = 0.35875 - 0.48829\cos\frac{2\pi n}{N} + 0.14128\cos\frac{4\pi n}{N} - 0.01168\cos\frac{6\pi n}{N} \tag{4}$$

BLACKMAN-NUTTALL WINDOW

$$w[n] = 0.36358 - 0.48918\cos\frac{2\pi n}{N} + 0.1366\cos\frac{4\pi n}{N} - 0.01064\cos\frac{6\pi n}{N} \tag{5}$$

COMMONLY USED MILLING TOOLS

These are some of the most common milling tool geometries used in the machining industry.

BALL END MILLING TOOL

Ball end milling tools are generally used for finishing processes.

Figure 37 – Geometry of a ball end milling tool.

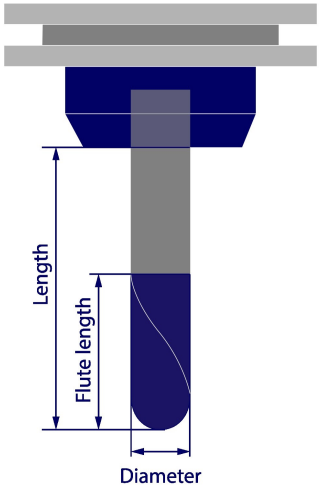

Source: **Company**' archive.

BULLNOSE MILLING TOOL

Bullnose milling tools are generally used for roughing processes. If a bullnose milling tool has corner radius of zero, that is, no corner radius, it is then name an end milling too.

Figure 38 – Geometry of a bullnose milling tool.

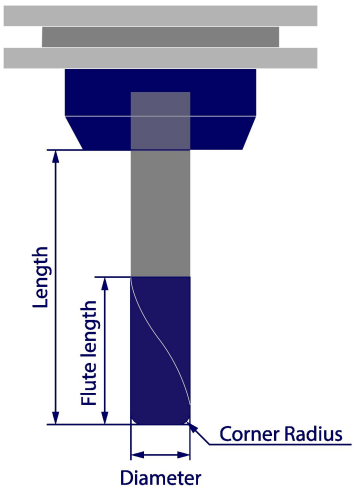

Source: **Company**' archive.

CHAMFERED MILLING TOOL

Chamfered milling tools are generally used for smoothing sharp edges by cutting with the tapered region.

Figure 39 – Geometry of a chamfered milling tool.

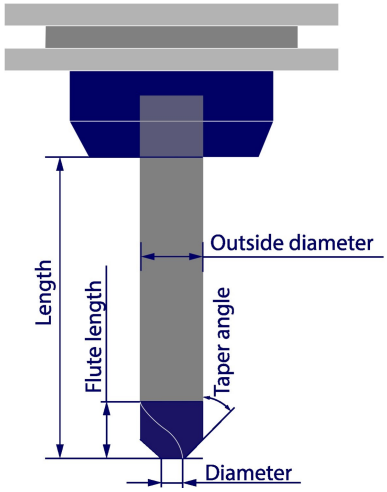

Source: **Company**' archive.

TAPERED MILLING TOOL

Tapered milling tools are can be used for both roughing and finishing. Its tip can be either flat, round, or have a corner radius, similar to a bullnose milling tool.

Figure 40 – Geometry of a tapered milling tool.

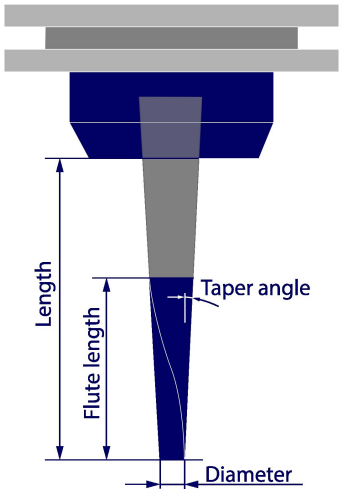

Source: **Company**' archive.